Ageing Research Reviews 49 (2019) 67–82

Contents lists available at ScienceDirect

Ageing Research Reviews

journal homepage: www.elsevier.com/locate/arr

Review

MRI-based evaluation of structural degeneration in the ageing brain: Pathophysiology and assessment

Lukas A. Grajauskas[a,b], William Siu[a,c], George Medvedev[a,d], Hui Guo[a,e], Ryan C.N. D'Arcy[a,b,f], Xiaowei Song[a,b,f,*]

[a] ImageTech Laboratory, Health Sciences and Innovation, Surrey Memorial Hospital, Surrey, British Columbia, Canada
[b] Department of Biomedical Physiology and Kinesiology, Simon Fraser University, Burnaby, British Columbia, Canada
[c] Department of Medical Imaging, Royal Columbian Hospital, New Westminster, British Columbia, Canada
[d] Department of Neurology, Royal Columbian Hospital, New Westminster, British Columbia, Canada
[e] Department of Medical Imaging, Tianjin Medical University General Hospital, Tianjin, China
[f] Health Sciences and Innovation, Surrey Memorial Hospital, Surrey, British Columbia, Canada

ARTICLE INFO

Keywords:
Brain ageing
Structural brain changes
MRI assessment
Pathophysiology
Neurodegeneration

ABSTRACT

Advances in MRI technology have significantly contributed to our ability to understand the process of brain ageing, allowing us to track and assess changes that occur during normal ageing and neurological conditions. This paper focuses on reviewing structural changes of the ageing brain that are commonly seen using MRI, summarizing the pathophysiology, prevalence, and neuroanatomical distribution of changes including atrophy, lacunes, white matter lesions, and dilated perivascular spaces. We also review the clinically accessible methodology for assessing these MRI-based changes, covering visual rating scales, as well computer-aided and fully automated methods. Subsequently, we consider novel assessment methods designed to evaluate changes across the whole brain, and finally discuss new directions in this field of research.

1. Introduction

Disorders of the ageing brain are one of the largest healthcare problems currently facing the world. Cognitive decline and dementia affects 13% of people older than 65 years and nearly 30% of those above 85 years of age, making them the most common cause of late life disability (Alzheimer's Association, 2016), and creating a substantial burden for patients and their families (Prince et al., 2013; World Health Organization, 2015). To address the impact of dementia, we need to better understand how the brain ages and degenerates.

Ageing is clearly associated with the accumulation of health problems, however these problems manifest heterogeneously across individuals and do not move forward in lockstep with the chronological age (Mitnitski et al., 2013). Because of this, individuals of a given age are not equally vulnerable to death or other adverse outcomes, but rather, their risk is associated with the rate of deficit accumulation, as multiple factors combine to overwhelm the bodies ability to repair itself (Rockwood and Mitnitski, 2011). Notably, this process can be particularly marked in the brain. High-level brain functions such as cognition rely on the integration of various structures, each of which can be affected by multiple health problems (Fjell, 2010). Even though it is possible for failure in brain function to occur due to the impact of a single element of degeneration, it is more likely that such failure will result from an interaction between multiple deficits that inevitably arise. Understanding how these changes occur and interact will allow us to better assess the risk of late-life cognitive decline and dementia.

Magnetic Resonance Imaging (MRI) has been used extensively to visualize these age related structural brain changes *in vivo* (Fjell, 2010).

Abbreviations: AD, Alzheimer's disease; ADNI, Alzheimer's Disease Neuroimaging Initiative; BMI, Body Mass Index; BALI, Brain Atrophy and Lesion Index; CAA, cerebral amyloid angiopathy; CADASIL, cerebral autosomal dominant arteriopathy with subcortical infarcts and leukoencephalopathy; CSF, Cerebrospinal Fluid; CT, computed tomography; FAST, FMRIB's automated segmentation tool; FLAIR, fluid attenuated inversion recovery; FSL, FMRIB software library; GSA, Global Cortical Atrophy Scale; MRI, Magnetic Resonance Imaging; MTA, medial temporal atrophy; MTAS, Medial Temporal Lobe Atrophy Scale; MCI, mild cognitive impairment; PVS, perivascular spaces; PDWI, proton density weighted image; SPM, Statistical Parametric Mapping; SVD, small vessel disease; T1WI, T1-weighted imaging; T2WI, T2-weighted imaging; UNIVRSE, uniform neuro-imaging of Virchow-Robin spaces enlargement consortium; WML, white matter lesion

* Corresponding author at: Fraser Health Authority, Head of MRI Program, Simon Fraser University ImageTech Laboratory, Surrey Memorial Hospital, 13750 96th Avenue, Surrey, British Columbia V3V 2Z1, Canada.
E-mail address: xiaowei.song@fraserhealth.ca (X. Song).

https://doi.org/10.1016/j.arr.2018.11.004
Received 12 May 2018; Received in revised form 8 November 2018; Accepted 21 November 2018
Available online 22 November 2018

Several changes visible on MRI such as white matter lesions (WMLs) and atrophy are clinically relevant and have each received a great deal of attention individually. Recently detection of "micro-scale" changes using MRI, such as dilated perivascular spaces, microbleeds, microinfarcts, and microvascular changes, has also become possible. These "micro-scale" changes can co-occur to produce additive impacts, and may precede more established clinical findings, therefore research into MRI based evaluation methods for these small changes has started to draw more attention (Boyle et al., 2013; Tosto et al., 2014; Iturria-Medina et al., 2016; Guo et al., 2017; Smith and Beaudin, 2018).

MRI methods designed to assess these changes have mostly focused on considering them individually, but correlations between different MRI-visible problems in the brain have been frequently reported (Longstreth et al., 2000; Schmidt et al., 2005; Zhu et al., 2010; Chowdhury et al., 2011; Potter et al., 2015a; Ding et al., 2017a,b). Despite these correlations, a method of integrating multiple coexisting changes is lacking. This avenue of research holds promise to paint a more comprehensive picture of the ageing process across the entire brain, and give us a better understanding of how multiple age related brain changes interact in a holistic manner.

In this article, we review several structural brain changes that are commonly seen in the ageing brain using MRI and discuss their impacts on brain ageing, with a focus on understanding their pathophysiology. We then describe the established methods used to assess these brain changes, consider new methods designed to evaluate changes across the whole brain, and finally discuss future research directions of the field.

2. Common structural changes in the ageing brain

Table 1 summarizes several common structural changes in the ageing brain, while examples of these changes are provided in Figs. 1 and 2 (Table 1; Figs. 1 and 2).

2.1. Atrophy

Among the most common and widely recognized changes in the ageing brain is "brain atrophy" or "cerebral atrophy". These terms refer to morphological alterations in the brain caused by a reduction in brain parenchymal tissue volume. As the tissue is lost, there is a consequential enlargement of ventricles, sulci, and other cerebrospinal fluid (CSF) spaces. Atrophy affects both grey and white matter, and while "global atrophy" often occurs in ageing, shrinkage can often be localized, leading to "focal atrophy", especially in disease pathologies.

While atrophy is nearly ubiquitous (Peters, 2006), its extent varies across individuals (Takeda and Matsuzawa, 1985), and it is seen at higher rates in patient populations (*e.g.*, dementia), when compared to normal ageing. Though the rate of atrophy varies across regions, it has been estimated that after age sixty, the total parenchymal volume loss progresses at a rate of approximately half a percent of the total brain volume per year (Enzinger et al., 2005; Hedman et al., 2012; Sigurdsson et al., 2012). The exact trajectory that atrophy takes is not completely clear as methodological differences between studies has prevented consensus. The differences include the use of different methods of quantifying atrophy (*e.g.*, visual rating or automated assessment), different follow-up periods, and different ages and co-morbidities present in the study population. Many studies also use cross-sectional designs and thus are unable to truly account for change over time in the individual. In addition, a biased sample could occur when a study uses a cohort from a dataset intended to study a specific disease.

Even though a consensus has not been reached, it has been shown that atrophy accelerates with age in certain brain regions including the entorhinal cortex, hippocampus, putamen, and precentral gyrus (Jiang et al., 2014), whereas it shows a linear trajectory in other regions including the amygdala, thalamus, nucleus accumbens, and caudate (Walhovd et al., 2005). It has also been shown that while regional atrophy rates may plateau in normal ageing after the age of 80, atrophy may continue unabated in AD (Schuff et al., 2012). Given the knowledge gaps, there is need for further research to comprehensively understand the trajectories of atrophy in different regions in the brain, and for populations with normal ageing and different disease conditions.

Atrophy patterns can also vary significantly between individuals of the same cognitive group. A recent study has reported multiple atrophy sub-types, *i.e.*, unique patterns of cerebral degeneration, in people diagnosed with AD (Ferreira et al., 2017). Searching for a common pattern of atrophy may be difficult given the considerable heterogeneity of brain atrophic changes even in older adults undergoing normal ageing (Raz et al., 2010). Dividing subject groups into subgroups based on spatial patterns and trajectory of atrophy may be needed to better account for individual differences and better uncover how different changes of brain function and atrophy are correlated. However, care must be taken as dividing samples into smaller groups may reduce statistical significance.

With respect to pathophysiology a combination of factors is thought to underlie cerebral atrophy including a loss of myelinated nerve fibers (Pakkenberg et al., 2003), a reduction of dendrites and synapses (Peters et al., 1998; Barnes, 2003), and even the death of neurons in their entirety (Anderton, 2002; Raz, 2004). The loss of glial cells is not thought to contribute to cerebral atrophy (Pakkenberg et al., 2003). While all of these aspects of degeneration seem to occur to some extent in the idiopathic cerebral atrophy seen in normal ageing, the relative contribution of each process can vary by disease (Regeur et al., 1994; Oster et al., 1995; Wegner et al., 2006).

Due to the varied functions of the brain regions affected, atrophy in each region will impact different aspects of cognition. For instance, atrophy in the prefrontal cortex manifests functionally as a decline in speed of processing, working memory, and cognitive control (Raz, 2004). The medial temporal lobe, which includes the hippocampus and entorhinal cortex, is central to long term memory, and atrophy here is strongly linked to memory loss and Alzheimer's type dementia (Squire and Zola-Morgan, 1991).

Risk factors associated with atrophy include cardiovascular problems, such as increased systolic blood pressure variability (Goldstein et al., 2002), raised systolic blood pressure (Taki et al., 2004), and hypertension (Kalmijn et al., 2000; Swan et al., 2000) as well as cardiovascular and cerebrovascular disease (DeCarli et al., 1999). Cerebral atrophy has also been associated with high body mass index (BMI), high alcohol intake, APOE4 allele, and white matter lesions (Enzinger et al., 2005).

2.2. Lacunes

The term "lacune" describes fluid-filled cavities seen in subcortical areas, generally 3 mm – 15 mm in diameter (Wardlaw et al., 2013). As they were originally thought to be healed infarcts, early literature often refers to these as "lacunar strokes" or "lacunar infarctions". However, subsequent research has shown these cavities are not always ischemic in origin but can also result from a healed small hemorrhagic event (Caplan, 2015). Therefore, it has been suggested that simply using the term "lacune" or "lacune of presumed vascular origin" is more accurate (Shi and Wardlaw, 2016).

Lacunes are commonly seen in older adults, though estimations of their prevalence vary based on the methodology of the study. A review of a number of studies found a range of reported prevalence, with lacunes seen in 8% to 28% of subjects (Vermeer et al., 2007), though a great deal of this variance can be explained by differing average age of the samples and the challenge of differentiating lacunes from perivascular spaces (PVS). Many studies only classify lacunes as findings between 3–15 mm in size, but others use differing size boundaries, contributing to this discrepancy in results (Vermeer et al., 2007). An increasing prevalence of lacunes has been reported as participants advanced in age (Vermeer et al., 2007), with one study finding new lacunes appeared in 3% of subjects every year, with incidence increasing

Table 1
Summary age-related brain changes commonly seen on anatomical MRI.

Change visible on MRI	Pathophysiology	Prevalence	Anatomical Distribution	Impact	Risk Factors	Best MR sequence to view change
Atrophy	Loss of myelinated nerve fibers, reduction of dendrites and synapses, or death of neurons	Near ubiquity in the normal ageing process, and increased (focal atrophies especially), in diseased populations	Seen across entire brain *e.g.*, frontal lobe in normal ageing, with differential atrophy patterns occurring in disease states	Variable impacts depending on location and severity, *e.g.*, medial temporal lobe atrophy on short-term memory	Variability in systolic blood pressure and raised systolic blood pressure, hypertension, high body mass index (BMI), high alcohol intake, APOE4 allele	T1WI, T2WI, T2-FLAIR optimal, T2*GRE possible
Lacunes	Luminal occlusion or atherosclerosis resulting in ischemic, microhemorrhage, or edema damage	8% to 28% in samples of normal elders. Increased prevalence in diseased populations	High prevalence in the basal ganglia areas: putamen, caudate; also in thalamus, pons, internal capsule, corona radiata, and cerebral white matter	Associated with gait disturbances, cognitive impairment, dementia, and depression	Age, ethnic factors, cardio- and cerebro-vascular, and metabolic factors; *e.g.*, diabetes mellitus	T2WI optimal, T1WI and T2-FLAIR possible
White Matter Lesions	Gliosis, demyelination, microcytic infarctions, and ischemic changes.	Estimates range from 5% to 90+% depending on sample	Periventricular lesions adjacent to the ventricles; punctuate and confluent lesions first in the frontal lobes, then other cortical regions.	Associated with cognitive and emotional dysfunction; falls, depression, dementia	Arterial hypertension, smoking, and stroke	T2-FLAIR optimal, T1WI and T2WI possible
Dilated Perivascular Spaces	Focal atrophy the tissue surrounding cerebral vasculature, gliosis, obstructed drainage of interstitial fluid, altered vascular wall permeability perivascular demyelination, and loosening of the arterial adventitia	Estimates range from 7% to 40% depending on sample and assessment procedures	Typically symmetrically distributed; common in the ventral aspects of the basal ganglia (may not represent pathology); also seen in the centrum semiovale along the path of penetrating pial arteries, and in the midbrain	Associated with cognitive decline, cerebral small vessel disease, lacunar strokes, multiple sclerosis, lupus and Alzheimer's disease	Cardiovascular risk factors, such as hypertension	T2WI optimal, T1WI and T2-FLAIR possible
Microinfarcts	Cortical: likely cerebral amyloid angiopathy (CAA); subcortical: atherosclerotic pathology	Estimates range from 3% to 43%	Occur throughout the brain, more likely in areas by major arteries, and cerebral cortex	Associated with executive impairment, Alzheimer's and vascular dementia	Cardiovascular risk factors, such as arteriosclerosis	T2 FLAIR optimal, T2WI possible
Microbleeds	Hypertensive vasculopathy, and CAA	Estimates range from 11.1% to 23.5%	Hypertensive vasculopathy in the basal ganglia, thalamus, and the infratentorial chamber; CAA in the cortical structures	Associated with executive impairment, haemorrhagic and ischemic strokes, white matter changes	Cardiovascular risk factors, such as hypertension	T2*GRE necessary

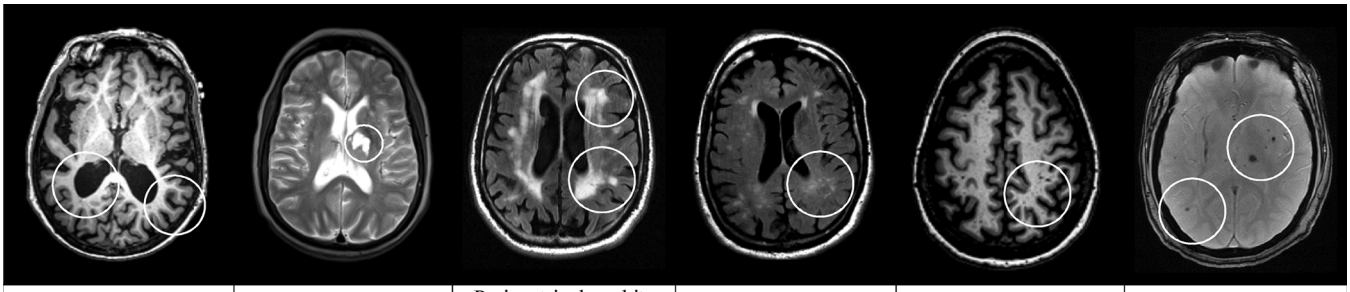

Fig. 1. Examples of age related structural brain changes viewed using 3 T MRI and appropriate sequences.

with age (Vermeer et al., 2003b). Some studies reported the prevalence of lacunes was as much as 40% higher in women that in men (Vermeer et al., 2002).

In the ischemic manifestation of lacunes, two pathologies are theorized to underlie the ischemia: luminal occlusion, and atherosclerosis. Lacunes often occur in areas supplied by the penetrating arteries where collateral circulation is minimal. Therefore pathology that narrows or blocks these, or upstream arteries, will lead to small areas of ischemia, and subsequently lacunes. One suggested pathology, luminal occlusion, can take place because of encroachment into the lumen by the thickening of the arterial walls, caused by disorders such as lipohyalinosis, cerebral amyloid angiopathy (CAA), or any other occlusive disease. Another pathology is the obstruction of the penetrating artery by an upstream atherosclerotic plaque in the parent artery (Caplan, 2015). Embolisms are generally not a cause of ischemia in these arteries (Boiten and Lodder, 1991). Haemorrhagic events can also result in lacunes, as well as edema resulting from increased vascular wall permeability (Rosenberg et al., 2001).

Lacunes are most often found in the basal ganglia, specifically the putamen and caudate. They also appear in the thalamus and pons, and within white matter structures such as the internal capsule corona radiata, as well as in the cerebral white matter (Caplan, 2015; Lammie, 2000).

Lacunes have often been considered clinically benign because of their high prevalence in the aged, and the lack of acute affects. However, lacunes have been shown to be present in larger numbers in elderly individuals with gait disturbances, cognitive impairment, dementia (Snowdon et al., 1997; Vermeer et al., 2007, 2003b), and depression (Yamashita et al., 2002). In particular, one major longitudinal MRI ageing study, the Rotterdam Scan Study, found that the presence of lacunes was linked with a 50% increased in the risk of dementia (Vermeer et al., 2003a).

Lacunes are sometimes classified as a part of “small vessel disease” (SVD), as their pathology stems from disorders of the small vasculature in the brain. SVD also encompasses white matter lesions, microbleeds, and microhemorrhage. However, this disease category is relatively non-specific, as several pathophysiological processes affect the small vessels, and the categorization refers simply to the structure effected, rather than the underlying pathophysiological processes at play. The category spans arteriosclerotic and inflammatory diseases, venous collagenosis, cerebral amyloid angiopathy (Pantoni, 2010), and genetic disorders such as CADASIL (Cerebral Autosomal Dominant Arteriopathy with Subcortical Infarcts and Leukoencephalopathy) (Chabriat et al., 2009), a heritable stroke disorder that is the result of a mutation in the Notch3 gene (Joutel et al., 1996). Depending on the processes at play, these underlying pathologies can differentially lead to lacunes, WMLs, microbleeds, or microhaemorrhage (Pantoni, 2010). The contribution of each process is discussed in the appropriate section of this review, based on the MRI visible findings.

2.3. White matter lesions

White Matter Lesions (WML) refer to patches of abnormal signal intensity seen in the brain’s white matter. These are thought to be linked to vascular changes and ischemia in the ageing brain. They can also be referred to as “Leukoaraiosis”, or “White Matter Hyperintensities” because of their appearance as patches of hyperintensities on CT and in T2-weighted imaging (T2WI).

WMLs have been shown to increase with age, and depending on the methodology of the study, prevalence of WMLs in elderly individuals can range from 5% to above 90% (Breteler et al., 1994; Grueter and Schulz, 2012; Launer et al., 2006; Vernooij et al., 2007; Wen and Sachdev, 2004). This large range of estimates is largely due to differences in ages and co-morbidities present in each sample, but methodological differences also contribute as some studies use visual rating scales while others use more quantitative methods (Galluzzi et al., 2008). Use of lower field strength may also lead to a smaller estimation of WML prevalence (Guo et al., 2014b), and different thresholds to consider WMLs present contribute to this inconsistency. For instance, the Rotterdam Scan Study threshold is greater than 6 ml of subcortical WMLs (Cees De Groot et al., 2000), while the CASCADE study used a threshold of 1.88 ml (Launer et al., 2006). Despite the different estimations, it is certain that their prevalence is much greater in the elderly than in younger populations (Hopkins et al., 2006), and is seen to increase exponentially between timepoints in longitudinal studies of the aged (Galluzzi et al., 2008).

WMLs have been traditionally classified into two different distributions: periventricular white matter lesions, and deep white matter lesions (Fazekas et al., 1993), each of which are thought to reflect a different underlying pathophysiology (Galluzzi et al., 2008). Periventricular lesions are seen in the white matter adjacent to the ventricles. Deep white matter lesions typically appear in the white matter of the frontal lobes first, and then progress to the parietal and occipital lobes (Galluzzi et al., 2008). Only in the most severe cases will the temporal lobe be affected (Grueter and Schulz, 2012). (Fig. 3, Panel A)

Periventricular WMLs directly border the ventricles and can be further subdivided into two categories. The first category usually appears as a smooth “cap” or “halo” surrounding the ventricle, which may reflect gliosis and demyelination (Kim et al., 2008), stemming from a breakdown of the ependymal lining which leads to “infiltration of water among the axons” (Fazekas et al., 1993). The second type seen are “patchy” lesions with more irregular borders surrounding the ventricle, which may be caused by ischemic changes, more similar to punctuate and confluent lesions (Kim et al., 2008; Thomas et al., 2003; Van Swieten et al., 1991).

Deep white matter lesions also have two subdivisions: punctuate,

and confluent. These may represent progression of a degenerative process, though some differing processes may be at play. Punctuate lesions are round with smooth boundaries, smaller than 5 mm, with multiple lesions seen in each patient. These have a less defined etiology, and may reflect microcystic infarctions (Thomas et al., 2002), perivascular alterations, or lack a defined pathology (Fazekas et al., 1993; Kim et al., 2008). Confluent WMLs are usually classified as lesions larger than 5 mm with irregular borders, which appear to arise from the confluence of smaller lesions. These are attributed to small vessel disease, where arteriolosclerosis narrows the lumen of cerebral arteries, causing mild ischemia, and leading to damages to the surrounding neural tissues. This damage ranges from demyelination and edema in its mild form, to gliosis and axonal destruction in severe cases (Pini et al., 2016).

WMLs are very prevalent and are seen even in the expected degenerative trajectories of healthy ageing. As a result, they have traditionally been thought to be benign (Kuo and Lipsitz, 2004). However, given it can be a precursor to stroke and other cerebrovascular diagnoses, considerable research effort has been made to understand the risk factors of WML. WMLs have been shown to be associated with arterial hypertension, smoking, and stroke (Barber et al., 1999; Leys et al., 1999; Longstreth et al., 1996; O'Brien et al., 1996). Additionally, WMLs are seen to be related to cognitive (Cees De Groot et al., 2000; Longstreth et al., 1996) and emotional (Cees De Groot et al., 2000; O'Brien et al., 1996) dysfunction. In particular, WMLs have been associated with falls (Briley et al., 1997), depression (Howard et al., 1995), urinary incontinence (Sakakibara et al., 1999), and depressive symptoms (Godin et al., 2008). Furthermore, research has shown that increased white matter lesion volume is predictive of the development of Alzheimer's disease (Brickman et al., 2012, 2015; Lindemer et al., 2015; Prins et al., 2004).

Though the traditional classification has divided WMLs into the two categories mentioned, newer work has used computer-based lesion mapping methods to look more closely at how the location of lesions connects to clinical outcomes. As could be expected, lesions have been shown to negatively impact the function of the area in which they are found. For instance, lesion load in the frontal horn correlates with executive dysfunction, lesions in the white matter junctions adjacent to the posterior horns of the lateral ventricles correlates with memory dysfunction, and lesions in the upper deep white matter—which includes the corticospinal tract—correlates with motor dysfunction (Lampe et al., 2017)

Furthermore, different lesion locations, which may reflect different underlying pathophysiologies, have been shown to be correlated with different severities of clinical impairment. Using principal component analysis, Duchesnay et al. (2018) showed that lesions in the pyramidal tracts and forceps minor were associated with more severe forms of impairment, and that this pattern was also associated with increased lacunes and brain atrophy. In contrast, lesions in the anterior temporal poles and superior frontal gyri were associated with milder forms of disease. These findings tie in well with the earlier consensus that periventricular WMLs are particularly associated with severity of cognitive impairment in demented patients (Bracco et al., 2005). However, even with these anatomical distributions, the role white matter plays in connecting brain areas means that WMLs can impair important functions, such as frontal lobe function, regardless of their location (Tullberg et al., 2007). These lesions may be even more destructive later in life when white matter volume begins to shrink due to cortical atrophy (Double et al., 1996)

2.4. Dilated Perivascular Spaces

This pathological change has classically been referred to as "dilated Virchow-Robin spaces" but terminology has shifted to favour the more physiologically informative name "dilated perivascular spaces". While perivascular spaces exist in healthy individuals, they are too small to be visible using current neuroimaging technology, and therefore they will only be visible when pathologically dilated. Thus, literature usually refers to their pathologically dilated manifestation simply as "Perivascular Spaces" (PVS). To align our terminology with the field, we will use the terms "perivascular spaces" or "PVS" to denote the pathological change. When numerous PVS appear together in the striatum, it can be referred to as état criblé, or status cribrosum (from Latin "cribrum", which means sieve). Because PVS lie parallel along the course of vessels, they can appear as small circular, oblong, or even linear cysts in MR images, depending on the slice orientation. These findings will have a similar signal intensity to CSF. Though there is no standard definition, PVS are generally classified as having a diameter smaller than 3 mm, as findings larger than this are more likely to be lacunes.

A number of studies show that PVS increase in prevalence with age (Satizabal et al., 2013; Zhu et al., 2010). Although this trend is still present in cognitively normal individuals, PVS are more prevalent in individuals diagnosed with Alzheimer's disease (Chen et al., 2011). While the increase with age is clear, there is little agreement about the exact prevalence of PVS in the population, as disagreement surrounding their classification and methodological issues stemming from different neuroimaging technologies leads to varied estimates in the literature (Ramji et al., 2017; Shi and Wardlaw, 2016). Their small size can make them difficult to view on 1.5 T images, which may lead to underestimation in some studies (*e.g.* Groeschel et al., 2006), and though the general definition for size is smaller than 3 mm, other studies may use a different size threshold (*e.g.* Chen et al., 2011). Additionally, some groups have included several MRI sequences in order to help gain specificity in differentiating PVS from lacunes (*e.g* Wang et al., 2012; Wuerfel et al., 2008), and some groups do not consider PVS in the basal ganglia to be pathological (*e.g.* Guo et al., 2014a,b).

In healthy individuals, perivascular spaces exist between cerebral arteries or veins, and the pia mater that surrounds them. While most studies do not differentiate periventricular and periarterial PVS, it appears that most findings investigate PVS surrounding arteries. However, the arterial and venous PVS have slightly different proposed functions, so more effort should be made to differentiate the two (Ramirez et al., 2016). Both types of spaces are thought to act in a similar manner to the lymphatic system, which is not present in the brain, with extracellular fluid being drained from the brain through perivascular spaces (Abbott, 2004; Schley et al., 2006). There is still some debate about the precise pathophysiology of PVS dilation (Ramirez et al., 2015), but the main hypotheses include focal atrophy of the surrounding tissue (Barkhof, 2004), gliosis (Shiratori et al., 2002), and obstructed drainage of interstitial fluid (Homeyer et al., 1996; Weller et al., 1992).

Typically, PVS are seen in three main areas in the brain and are generally found in a symmetrical distribution. (Fig. 3, Panel B). The most common location is in the ventral aspects of the basal ganglia, surrounding the lenticulostriate arteries as they enter through the anterior perforated substance (Jungreis et al., 1988). However, this may not represent a pathological presentation, because PVS are seen here with very high prevalence even in young individuals, and the dilation may be the product of the different anatomy of the perivascular spaces in the basal ganglia (Kwee and Kwee, 2007). A second location occurs in the centrum semiovale, a white matter tract above the lateral ventricles and corpus callosum. Particularly, PVS here appear along the path of penetrating pial arteries. Finally, PVS are often present in the midbrain (Ramji et al., 2017).

Across all of the anatomical distributions that are seen, increases in visible PVS are associated with cognitive decline (Hurford et al., 2014; Weller et al., 2015), dementia (Ding et al., 2017a; Zhu et al., 2010), cerebral small vessel disease (Potter et al., 2015b), multiple sclerosis (Favaretto et al., 2017), and lupus (Miyata et al., 2017).

As the lack of uniformity in the classification of PVS has led to difficulties in generalizing results between research studies, a recent initiative, the "Uniform Neuro-Imaging of Virchow-Robin Spaces

Enlargement" (UNIVRSE) Consortium, has been formed with the hopes of standardizing definitions and pooling data to create samples of larger size (Adams et al., 2015).

2.5. Microscale changes: microinfarcts and microbleeds

A series of changes have also been noted that are beyond the current detection threshold of conventional clinical neuroimaging techniques, although research has increasingly implicated these changes in the process of brain ageing. These require ultra-high field MRI (usually 7 T) or specialized sequences to be visualized, tools not available to the majority of clinicians or scientists. However, as technology progresses, these tools may become more available.

Two of the main findings that these tools allow us to view are microinfarcts and microbleeds. Microinfarcts are tiny areas of necrotic tissue resulting from prolonged ischemia affecting brain parenchymal tissue. Microbleeds are the haemorrhagic counterpoint to this and are seen as tiny areas of blood break-down products within the brain. The range of size cut-offs used to classify these in the literature has varied (Brundel et al., 2012), but they can most easily be considered infarcts that cannot be visualized using conventional MRI. The creation of more precise criteria is complicated by differences in visualization caused by different choices in imaging parameters (van Veluw et al., 2017).

Both of these microvascular changes are prevalent in the ageing population, with MRI based estimates of microinfarcts ranging from 3% to 43% (Brundel et al., 2012) and microbleeds ranging from 11.1% to 23.5% (Greenberg et al., 2009), with studies showing increasing prevalence with age (Vernooij et al., 2008). Again, differing sample characteristics leads to the variability in estimations, and there is little standardization in the size classification of these findings, with some studies using a threshold as small as 50 μm to 400 μm (White, 2009) and others accepting findings as large as 5 mm (Haglund et al., 2006; Soontornniyomkij et al., 2010).

Microinfarcts can occur anywhere in the brain, though some studies have found they are more likely to occur in watershed areas, and the cerebral cortex (Brundel et al., 2012). Microinfarcts seen in the cortex are more likely to stem from cerebral amyloid angiopathy, while subcortical microinfarcts tend to stem from atherosclerotic pathology (van Veluw et al., 2017).

Microbleeds are generally seen in two spatial distributions, each stemming from a different underlying pathologies (Greenberg et al., 2009). Microbleeds stemming from hypertensive vasculopathy are usually seen in the basal ganglia, thalamus, brainstem, and cerebellum (Fazekas et al., 1999), and microbleeds stemming from cerebral amyloid angiopathy (CAA) are seen with a lobar distribution, and less frequently, in the cerebellum (Knudsen et al., 2001).

There are several underlying causes that can lead to microinfarcts and microbleeds, many of which can exist simultaneously in a single patient. Microinfarcts throughout the brain can result from cerebral amyloid angiopathy, which is the buildup of amyloid protein in vessel walls, as well as arteriosclerosis, microemboli, and hypoperfusion (van Veluw et al., 2017). Microbleeds can result from hypertensive vasculopathy (Fazekas et al., 1999; Knudsen et al., 2001), which occurs when hypertension causes structural changes in the vessel walls (Park, 2014). Microbleeds can also result from cerebral amyloid angiopathy (Franz Fazekas et al., 1999; Knudsen et al., 2001).

Because the changes are so small, there is usually little acute impact. However, there is evidence that they play a role in functional decline. Evidence shows that patients with more microbleeds in the frontal lobe and basal ganglia had greater impairment in executive control than patients without lesions (Werring et al., 2004), and that patients with more microbleeds had a higher risk of cognitive impairment and death (Greenberg et al., 2004). Microinfarcts are associated with diagnoses of AD and vascular dementia (Brundel et al., 2012), and microbleeds may predict future haemorrhagic (Greenberg et al., 2004) or ischemic strokes (Soo et al., 2008), and are associated with disability in CADASIL (Oberstein et al., 2001).

Contrary to other neuropathological findings, histopathology may not provide the gold standard for assessment of these changes. Their miniscule scale means they could be entirely contained in even the thin slices used in histopathology, and usual histopathological examinations do not cover the entire brain in microscopic detail. Contrary to this, high field MRI is capable of imaging the entire brain, and can be captured with higher in-plane resolution than the slices used in histopathology (Greenberg et al., 2009).

3. Conventional methods of assessing structural brain changes using MRI

Several MRI based assessments methods have been developed to understand the common age-related changes that occur in the brain. These allow clinicians and scientists to assign a quantitative score to the images, permitting standardized comparisons and the tracking of changes. Humans are very effective at evaluating complex images, so the first methods were simply manual evaluations, which are simple to employ, and a good fit for the clinical environment. However, recent increases in computational power have allowed for the development of new computer aided techniques. These can be employed to assess large datasets and can be much more quantitative, less subjective, and more consistent than manual ratings. However, even these are not perfect, and a great deal of development is going into computer-based methods of assessing MR images. We will discuss manual evaluation methods, methods which combine human raters and computers, as well as some fully automated methods. Each methodology has its relative strengths and weaknesses, which must be weighed against one another when deciding upon their implementation.

3.1. Manual rating scales

Humans beings are currently unparalleled in their ability to assess complex images, and so many scales rely on human raters to evaluate images in a standardized manner, allowing the assignment of scores which can be compared across time points or locations. While a few neurodegenerative changes have widely accepted rating scales, most have multiple published rating methods, each with purported advantages and limitations and often with unknown generalizability beyond the data which the scale was applied to. The problem of competing scales is especially rampant in changes considered less relevant to clinical practice, which therefore have less unified demand for standardization. Here we review a few manual rating scales for several prominent changes. This is by no means a comprehensive list but is instead intended to illustrate the methodology currently in use for the assessment of age related brain changes. Table 2 lists established MRI based rating scales used for the assessment for structural brain changes (Table 2).

3.1.1. Atrophy

Long considered a hallmark of age related degeneration, atrophy is easily visualized, and thus numerous standardized rating scales have been created to assess it. In clinical settings, atrophy is often considered in an unstructured manner, but it has been shown that the application of a structured rating scale improves the reliability of assessment, as well as the ability to diagnose different conditions (Harper et al., 2016). Several different rating scales have been created to assess global atrophy, as well as atrophy in specific areas.

Among the age-related neuroimaging scales that currently exist, one that has found widely accepted use is the Medial Temporal Lobe Atrophy Scale (MTAS), also known as the Scheltens Scale, which is used to evaluate the degree of atrophy in the medial temporal lobe (Fig. 4). Atrophy here has been shown to be a hallmark symptom of AD, and therefore the scale is often used to differentiate Alzheimer's type dementia from other dementias. To employ the scale, a rater assesses a T1

Table 2
Structural brain changes and several well established visual rating scales used to assess them.

Structural Change	Rating Scale	Description	First Introduced and Key Papers (year)
Atrophy	Medial Temporal Atrophy Scale	Evaluates atrophy in the medial temporal lobe. Rater uses a T1 weighted coronal slice to rate three elements of medial temporal lobe degeneration: the width of the choroid fissure, the width of the temporal horn, and the height of the hippocampal formation.	Scheltens et al. (1995)
	Global Cortical Atrophy Scale	Assesses 13 areas in the brain, with separate ratings assigned for each of these areas in both hemispheres.	Pasquier et al. (1996)
	The Koedam Score, or posterior atrophy score	Uses all three planes to assess seven structures, giving a quantification of parietal atrophy.	Koedam et al. (2011)
	Anterior Temporal Scale	Focuses on atrophy in the frontotemporal region, and uses two standardized slices to rate three areas, with the aim of assessing frontotemporal dementia.	Davies et al. (2006)
White Matter Lesions	The Fazkas scale	Assesses the presence of WML across the entire brain. The scale rates the severity of lesions on a scale of 0 (no deficit) to 3 (maximal deficit) in periventricular white matter and deep white matter.	Fazekas et al. (1987)
	Scheltens scale for WMLs	Rates areas of the brain individually, and adds the basal ganglia and infratentorial regions, territory not included in the Fazekas scale.	Scheltens et al. (1993)
	Age-Related White Matter Changes (ARWMC) Scale	Requires two sets of images, a T2WI, and a proton density weighted image (PDWI) or fluid attenuated inversion recovery (FLAIR) image. Five different areas are rated in the left and right hemispheres separately, including a rating of the basal ganglia	Wahlund et al. (2001)
Dilated Periventricular Spaces	Uniform Neuro-Imaging of Virchow-Robin Spaces Enlargement (UNIVRSE) Consortium Rating Scale	On an axial T2WI, the number of PVS between the sizes of 1 mm and 3 mm are counted in four regions: the hippocampus, and mesencephalon, which are assessed in their entirety, and the centrum semiovale and basal ganglia, which are assessed using a pre-defined slice.	Adams et al. (2015)
	Numerous scales used for individual studies without standardization	Various methods.	Maclullich et al. (2004), Patankar et al. (2005), Cumurciuc et al (2006), Groeschel et al. (2006), Chen et al. (2010), Zhu et al. (2010) and Potter et al. (2015a,b)
Whole Brain Evaluation of Multiple Age-Related Changes	Brain Atrophy and Lesion Index (BALI)	Assessed using T1 or T2 weighted 3D or 2D images; multiple categories of age related structural changes including white matter, atrophic, and small vessel deficits are assessed for severity across the entire brain in both supratentorial and infratentorial regions.	Chen et al. (2010), Zhang et al. (2011), Guo et al. (2014a,b) and Guo et al. (2017)

weighted coronal slice through the medial temporal lobe, with full view of the body of the hippocampus. Points from 0 (no deficit) to 4 (maximal deficit) are assigned to three areas: the width of the choroid fissure, the width of the temporal horn, and the height of the hippocampal formation (Scheltens et al., 1995). However this method does not have perfect specificity in relation to AD, as medial temporal lobe atrophy (MTA) can be seen in different forms of dementia (Barber et al., 1999).

Several other scales have also been created with different intentions. These include the Global Cortical Atrophy scale (GCA), also known as the Pasquier scale, which assess cortical atrophy as a whole (Pasquier et al., 1996). The GCA scale assesses 13 areas in the brain, with separate ratings assigned for each of these areas in both hemispheres. Another, the Koedam Score, or posterior atrophy (PA) score, uses all three planes to assess seven structures, giving a quantification of parietal atrophy, which has been shown to be a predictor of AD and is linked with other forms of dementia (Koedam et al., 2011). The Anterior Temporal (AT) scale (Davies et al., 2006; Kipps et al., 2007) focuses on atrophy in the fronto-temporal region, and uses two standardized slices to rate three areas, with the aim of assessing fronto-temporal dementia.

3.1.2. White Matter Lesions

White matter lesions can also be relatively easily viewed and rated using visual scales. The Fazekas scale for white matter lesions (Fazekas et al., 1987), is perhaps the most widely used method of evaluating WMLs. The scale assesses the presence of WMLs across the entire brain. The scale rates the severity of lesions on a scale of 0 (no deficit) to 3 (maximal deficit) in periventricular white matter and deep white matter, and a high Fazekas scale score is considered a risk factor for future degeneration and disability. However, the scale is relatively non-specific, as it does not strongly differentiate between risks of different types of dementia. Another commonly used scale is the Scheltens scale for WMLs (Scheltens et al., 1993). Arguing that the Fazekas scale only provided global information on the presence of WMLs rather than specific information on the anatomical distribution of WMLs, Scheltens et al. (1993) proposed a more detailed scale. This scale rates areas of the brain individually, and adds the basal ganglia and infratentorial regions, which are not included in the Fazekas scale. While this scale gives more detailed information on the distribution of WMLs, it is more time consuming to rate. Another scale, the Age-Related White Matter Changes (ARWMC) scale (Wahlund et al., 2001) requires two sets of images, a T2WI, and a proton density weighted image (PDWI) or fluid attenuated inversion recovery (FLAIR) image. Five different areas are rated in the left and right hemispheres separately, including a rating of the basal ganglia. A few other scales exist as well, and while no one scale has been shown to be superior to any of the others (Pini et al., 2016), simpler rating scales may be just as effective as complex ones when looking at the relationship between clinical factors such as cognition and physical performance, and WMLs (Gouw et al., 2006). Pantoni et al. (2002) gives an overview of some of the widely employed scales and calculates conversion coefficients to help compare ratings between them.

3.1.3. Perivascular spaces

Traditionally, PVS have been considered less clinically relevant, and so there is little standardization in terms of rating methodology. However, because of their connection to vascular pathology, there is increasing research interest. Because they are a newer research realm, most of the studies assessing the changes have proposed to use their

own rating scales (Chen et al., 2010; Cumurciuc et al., 2006; Groeschel et al., 2006; Maclullich et al., 2004; Patankar et al., 2005; Potter et al., 2015a, Zhu et al., 2010). This has allowed researchers to assess the severity and occurrence of PVS, but generalizing across studies can be difficult. Overall, the scales are similar, but differ along two axes. First they differ in their specificity of their PVS count, some giving a more exact number of PVS present, and others giving ranges instead (> 5 PVS = 1 point, 5–10 PVS = 2 points, *etc*). Second, they differ in the number of sub-regions assessed, with some combining large parts of the brain, and others dividing the brain into numerous sub-regions. This is a trade-off between the precision of the score, and the ease of use. More precise enumeration and more sub-regions lead to a more informative, but also more time-consuming scale. Studies also differ in the length to which they go to distinguish PVS from lacunes, with some studies simply using size and location (*e.g.* Chen et al., 2011), while other studies include multiple MRI sequences to make a more accurate assessment (*e.g.* Adams et al., 2013). In response to the lack of agreement on how to assess PVS, the UNIVRSE consortium created a review of the published literature in the research area, and proposed a single rating methodology for standard use, as described in Adams et al. (2015). It is yet to be seen whether this scale becomes the accepted norm, and if it has any clinical utility.

3.1.4. Lacunes, microbleeds, and microinfarcts

While these changes are often seen in the ageing brain, there has been little attempt to create a standardized rating system. Lacunes usually occur alone or in small numbers, and can therefore be easily noted in an unstructured manner. Microbleeds and Microinfarcts are still beyond the detection threshold of conventional MRI, and as such, visual rating scales have not been developed.

3.1.5. Challenges of MRI based visual rating

Historically, rating scales have played a very important role in clinical settings owing to their ease of application. For the same reason, rating scales are commonly employed in neuroimaging studies. However, these scales still suffer from the limitations of operator dependent error, and with the increase in large multicentre datasets available, human assessment is less equipped to handle images from thousands of individuals. Additionally, many neuroanatomical changes appear very similar when viewed using MRI, even when the changes stem from differing pathology. For example, it is often difficult to distinguish lacunes from PVS, as both are small punctuate changes (van Veluw et al., 2017). Making such distinctions is possible, but often require the use of multiple sequences, and advanced knowledge.

3.2. Computer aided volumetric assessment methods

3.2.1. Computer aided and semi automated methods

Computers have paved a new avenue to create precise quantitative measures of brain changes using volumetric methodologies. Though many current methods employ automation, volumetric methods can also rely strongly on manual input. Using a computer, a human will delineate the structure of interest by manually tracing its outline in subsequent slices on an MR image, and the computer then calculates the volume of the structure. Some methods also use a semi-automated technique, where a rater will manually select anatomical landmarks, and a computer program will use this to assist in defining the structure and calculating its volume (Keller and Roberts, 2009).

3.2.2. Fully automated methods

With increases in computing power and image processing capability, fully automated methods of creating volumetric measures of MRI images have also become prevalent. Using a standardized computer program reduces the issue of inter-rater and intra-rater reliability that exist in manual rating scales, as the same computer program can be used at multiple time points, and in multiple labs or clinics. Automated methodologies can also be applied by a researcher with less specialized knowledge about neuroanatomy, and it can be used to assess large datasets relatively easily (Keller and Roberts, 2009). As we see an increasing push to the creation of large multicentre datasets such as UK Biobank, Alzheimer's Disease Neuroimaging Initiative (ADNI) and the Human Connectome Project, automated methods are becoming increasingly important, as it is not feasible for human raters to assess the thousands of images in these large datasets. In large datasets such as these, some of the limitations of automated techniques may be outweighed by the need for efficiency. Automated methods have been shown to give a robust quantitative estimation of structures that can be easily delineated on MR images, such as grey matter, brain parenchyma, and ventricular volume (Keller and Roberts, 2009), but new methodologies have applied similar methodology on a number of deficits such as WMLs (Caligiuri et al., 2015) and dilated PVS (Ramirez et al., 2015), as well as other complex structures (Craddock et al., 2017).

However, while automated methods may be more reliable, they still have not achieved perfect detection capabilities, and they include elements that may reduce their validity relative to manual rating scales. These techniques rely greatly on image level data, and therefore, because of a lack of “top down information” about anatomy to make decisions, automated methods will be far more affected by imaging parameters. Artifacts and signal-to-noise issues will pose a problem, and if images are acquired with differing imaging parameters—as is often the case with large multi-centre datasets—the automated methodology will have problems comparing images collected with differing parameters. The analysis of smaller structures may be challenging with lower resolution images, or when there is low signal-to-noise ratio. Segmentation can also be difficult in parts of the brain such as the basal ganglia, where there is not a distinct delineation between nearby structures. Furthermore, some methodologies fit the acquired image to a standardized brain atlas, which can decrease the resolution and make the process more susceptible to partial volume errors (Keller and Roberts, 2009).

3.2.3. Application of Automated Assessment Methods

Of the brain changes considered, automated assessment of global atrophy, as well as that of white matter and CSF volume changes has been comparatively easy to develop and employ, owing to the relatively clear boundaries between grey matter, white matter, and CSF. Most widely employed open source MRI processing packages contain a segmentation tool that can be used to quantify tissue volume; SPM (Statistical Parametric Mapping) software has segmentation capabilities, and FSL (FMRIB Software Library) includes FMRIB's Automated Segmentation Tool (FAST) (Zhang et al., 2001). Though these are both open source, SPM does require a MATLAB licence. There are also stand alone segmentation tools each with their own methodologies. These include open source programs such as Freesurfer (Fischl, 2012), 3DSlicer (Fedorov et al., 2012), and ANTs (Avants et al., 2011), and others that combine open source and closed source tools such as BrainVISA (Cointepas et al., 2001). Several groups have also created their own processing methods based on a number of theories about image processing. The theoretical underpinnings of segmentation methodologies are beyond the scope of this review, but Angulakshmi and Lakshmi Priya (2017) gives a good introduction to the subject. Direct comparison between these segmentation methods is difficult, as individual groups may not make their algorithms publicly available, some algorithms may be more optimized for a specific use, and the larger open source libraries are often updated. The segmentation tools included in the commonly used software libraries are generally considered sufficient, though some groups unsatisfied with their capabilities have designed their own methods.

Open source automated segmentation techniques (Freesurfer, FSL’s FIRST, *etc*) have also been used for tracking focal atrophy, such as hippocampal atrophy. Due to the similarity in grey matter intensity

between the hippocampus and surrounding structures, this is a considerably more difficult problem, and a number of custom techniques have also been developed; Pini et al (2016) reviews some of these techniques.

Automated volumetric assessment of WMLs can present a challenge, as their borders may not always be sharply delineated. However, having the capability to localize WMLs at the voxel level can open new research avenues, such as the investigation of how patterns of WMLs correspond to observed symptoms, or whether WML patterns differ between healthy and pathological ageing (Griffanti et al., 2016). A number of methods for the automated segmentation of WMLs have been developed and have shown good results, though only a few are open source, and many were only trained on small datasets. (Caligiuri et al., 2015 reviews these). One open source tool, BIANCA (Brain Intensity AbNormality Classification Algorithm) (Griffanti et al., 2016) was introduced as part of FSL and is generally accepted as the leading methodology. While still considered "in testing", it is a step forward in the automated classification of WMLs.

Several attempts have been made to create an automated volumetric method of assessing PVS, however, much like manual rating scales, there is little agreement. There is particular difficulty assessing these small structures, but the increase in the use of 3 T scanners have made this easier (Hernández et al., 2013). In addition to this, a few studies have made use of 7 T images to segment images, giving a promising new avenue for development (Bouvy et al., 2014; Harteveld et al., 2016).

Though a number of techniques for segmenting structures and neurodegenerative changes have been developed, one must consider the aims of the project before choosing a methodology. Methods that allow for precise quantification of the volume of structures such as the hippocampus have useful applications in things such as genetic studies, where the techniques have led to the discovery of novel genes associated with hippocampal volume (Stein et al., 2012). However, existing methods still do not have sufficient ability to characterize or predict AD. In fact, some manual rating scales outperformed automated methods in their ability to predict which subjects categorized into the mild cognitive impairment (MCI) group would convert to AD (Varon et al., 2015), and have shown equivalent ability to differentiate HC, MCI, and AD patient groups based on hippocampal atrophy (Li et al., 2018). This suggests that rather than simply assuming the superiority of computational methodology, we should instead consider the relative advantages of each method in the context in which we are employing it. Automated methods have an advantage in large datasets where visual rating would be too labour intensive to be feasible, and while more precise tracking of a change may be useful in research settings, it is not always necessary.

4. Whole brain evaluation of multiple age-related changes

4.1. Connections between structural changes

While each of the age-related changes reviewed have a slightly different presentation, multiple changes are nearly always seen in the ageing brain as various systems in the brain degenerate at the same time. Although age related changes may manifest in different severities and patterns across individuals, most of these changes have been shown to be linked in their presentation across individuals. Underlying pathophysiology may have linked aspects that underlie different changes, and genetic and lifestyle risk factors can lead to greater risk for several different changes at once, leading to the accumulation of multiple deficits. Most of the studies that looked at more than one deficit found associations between the severity of the deficits they measured. Correlations were seen between the amount of atrophy and the amount of WMLs (Longstreth et al., 2000; Schmidt et al., 2005), between the number of PVS and the amount of WMLs (Ding et al., 2017a; Zhu et al., 2010), between the amount of WMLs and microbleeds (Chowdhury et al., 2011), between the amount of PVS and subcortical infarcts, microbleeds (Ding et al., 2017b), lacunes, and atrophy (Potter et al., 2015b). Furthermore, when multiple changes were seen together, they were more strongly associated with cognitive decline and risk of dementia (Zhang et al., 2012). Also, when several changes were looked at together, there was an increase in ability to predict decline (Appel et al., 2009; Prasad et al., 2011). For instance, in the prediction of AD, MTA is seen as the hallmark neuroimaging biomarker, but when measures of MTA are combined with other changes, such as WMLs (Appel et al., 2009; Prasad et al., 2011), cerebral atrophy (Jacobs et al., 2011), or both (Brickman et al., 2008), specificity and sensitivity can be increased.

Together, this points to the fact that though there are some hallmark neuroimaging findings that occur in the brain, they are interconnected, and considering them together paints a better picture of brain ageing and neurodegeneration. Further, though some changes have been considered sub-clinical findings in the past, the small impacts of multiple changes in combination can create a large cumulative impact on the complex system that is the human brain.

4.2. Whole brain evaluation methods

While there have been attempts to combine several scales or brain changes together in different studies, there are few existing scales that aim to combine a broad assessment of changes across the entire brain into one estimate. There is some work that has attempted to create a whole brain neurodegeneration tracking method for use with structural MRI. However, most of this work only considers atrophy across different areas as the biomarker of interest. Given that there are a number of other age-related changes that occur in the ageing brain, including them will give a more generalizable picture of brain ageing and neurodegeneration. There are currently a few methods that attempt to integrate multiple structural changes into a single measure that gives an overall picture of the state of the ageing brain.

Emerging approaches include one proposed by Park and Moon (2016), which suggested a methodology to integrate several visual rating scales across the entire brain and across multiple changes, but rather than assign a "score" to the level of degeneration, the system is used to help with the differential diagnosis of different dementias. For instance, if visual assessment is positive for medial temporal lobe atrophy and negative for WMLs, this suggests AD, while if the assessment is negative for medial temporal lobe atrophy and WMLs, but lobar microbleeds are present, this suggests CAA. Jang et al. (2015) has attempted to create a "comprehensive visual rating scale" (CVRS) for the assessment of multiple changes across the brain. This method is heavily weighted to an assessment of atrophy, with the inclusion of hippocampal atrophy, cortical atrophy, ventricular enlargement, and small vessel disease. This results in a "whole brain" score out of 30, with 23 points based on these atrophy categories, and only 7 allotted to the small vessel disease category which includes WMLs, lacunes, and microbleeds. While this approach is good in its consideration of multiple changes, the weighting away from SVD may be disadvantageous, as increasing evidence links vascular changes to dementia and other forms of neurodegeneration. The application of the CVRS showed good inter-rater and intra-rater reliability, was correlated with volumetric assessments, and was fast to rate. The CVRS has only been applied to one sample of 260 individuals to date, so the utility of the scale remains to be seen.

Additionally, there has been recent effort to create a method of assessing "brain age", but this differs somewhat from attempts to create a whole brain rating system for age-related neurodegeneration. Scales focusing on age-related neurodegeneration emphasize neuropathology and risks of cognitive impairment and other age-related disorders like dementias. In contrast, a brain age score attempts to quantify the integrity of a person's brain, based on a hypothetical trajectory of healthy ageing. These methods are usually based on automated methods, which

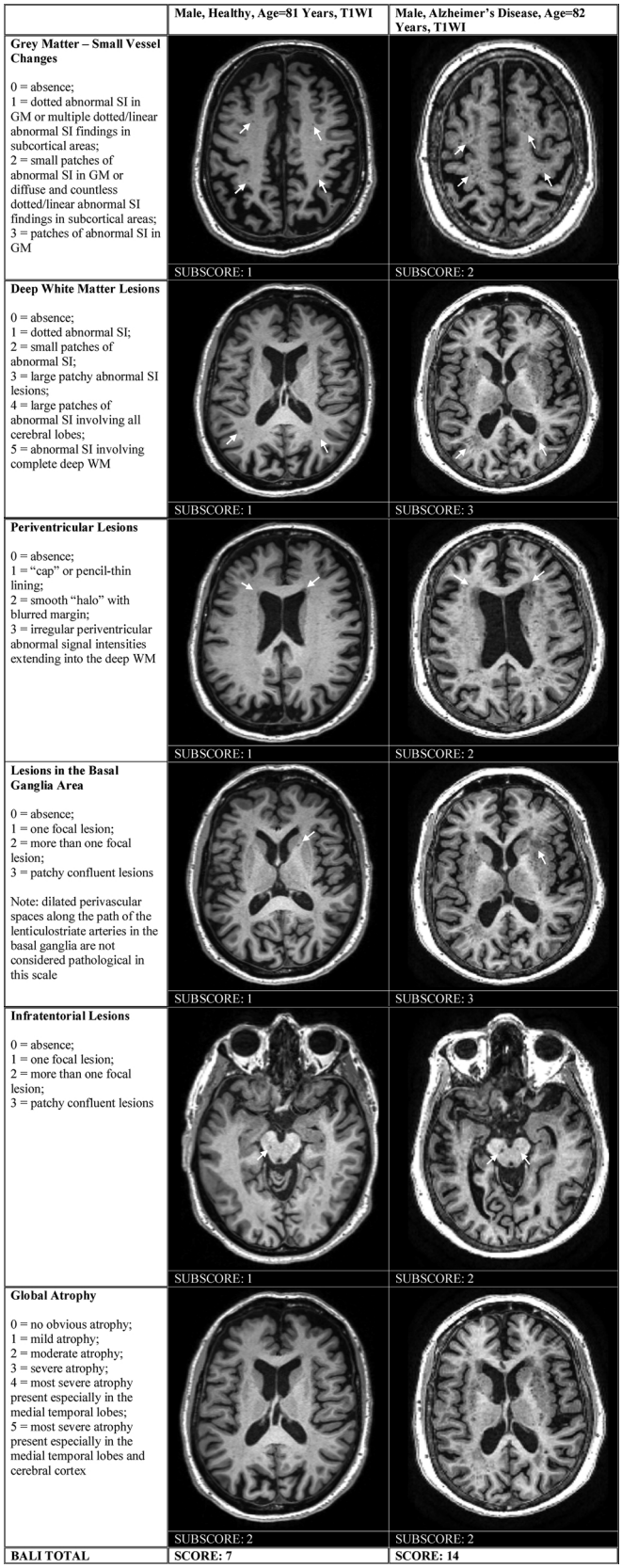

Fig. 2. Examples of whole-brain structural change assessment using the Brain Atrophy and Lesion Index.

are trained on large datasets to predict chronological age, and then applied to new data to give a "brain age", which may differ from actual chronological age based on the level of degeneration in the selected parameters. However, many of these rating scales focus exclusively on atrophy in different parts of the brain, with a few focusing on Diffusion Tensor Imaging (DTI) measures or connectivity maps (Cole and Franke, 2017).

The best developed method aiming to address this issue is the "Brain Atrophy and Lesion Index" (BALI). First proposed in 2010 (Chen et al., 2010), it is a visual rating scale that combines elements of several previously validated rating scales, and has the capability of assessing multiple domains simultaneously, giving a semi-quantitative measure of neurodegeneration across the entire brain. The scale has categories for seven neurodegenerative changes: Grey Matter Lesions and Subcortical Dilated Perivascular Spaces, Deep White Matter Lesions, Periventricular White Matter Lesions, Lesions in the Basal Ganglia and Surrounding Areas, Lesions in the Infratentorial Compartment, Global Atrophy, and Other Findings. Fig. 2 shows examples of brain structural health evaluation using the BALI (Fig. 2). Each area is given a semi quantitative rating on a scale of one to three, with scores of up to five possible in the Deep White Matter and Global Atrophy categories to account for ceiling effects (Grajauskas et al., 2018). For instance, within the Basal Ganglia sub-score of the BALI, the rater will give one point if there is only one punctuate lesion, two points if there are multiple punctuate lesions, and three points if there are patchy lesions. The scale is assessed using axial slices, and has been validated on both T1 and T2 weighted images. Use of only one of these common clinical sequences is sufficient, but if expert raters wish, additional specialized sequences can be included for a more detailed assessment (Guo et al., 2017) The scale can be applied quickly (less than 5 min.), which makes it a good fit for clinical settings or larger datasets, and has been validated for use by non-expert raters. Guo et al. (2014a) gives a standardized protocol for applying the scale, availing researchers and interested clinicians the resources to employ it.

A series of research studies have employed the BALI since its inception, applying it to rate MR images from over 3000 subjects drawn from multiple independent datasets from around the world, including in house datasets (Chen et al., 2010), ADNI, the Australian Imaging Biomarkers and Lifestyle Study of Ageing (AIBL) datasets (Song et al., 2017) as well as data collected at the Tianjin Medical University General Hospital (Guo et al., 2017). This work showed the BALI to be an effective measure which is well correlated with cognitive scores (Zhang et al., 2011), and promising for its ability to distinguish AD and MCI subjects (Zhang et al., 2012). While this scale has yet to see clinical implementation, it is the best existing example of an MRI based assessment method that attempts to quantify whole brain health through the evaluation of multiple structural changes in the brain.

Though they show promise, much work still needs to be done before any of these scales comes into the mainstream. Continued validation is required, and an increased focus on clinical implementation is needed to help the scales find use.

5. Discussion

In this review, we summarized the major aspects of age related neurodegeneration visible on MRI, covering well documented age-related brain changes as well as less clinically recognized brain changes that are receiving increasing focus. We discussed the current methodology available to assess these changes, covering a range of manual and automated rating scales, and comparing some of their relative weaknesses and advantages. Our review of these measures notes that they are generally focused on a single element of degeneration, leading to a gap in our ability to rate and assess the collective burden of multiple neurodegenerative changes across the entire brain. As we begin to understand the large degree that these changes interact in the ageing brain to produce negative outcomes, it is becoming clear that the

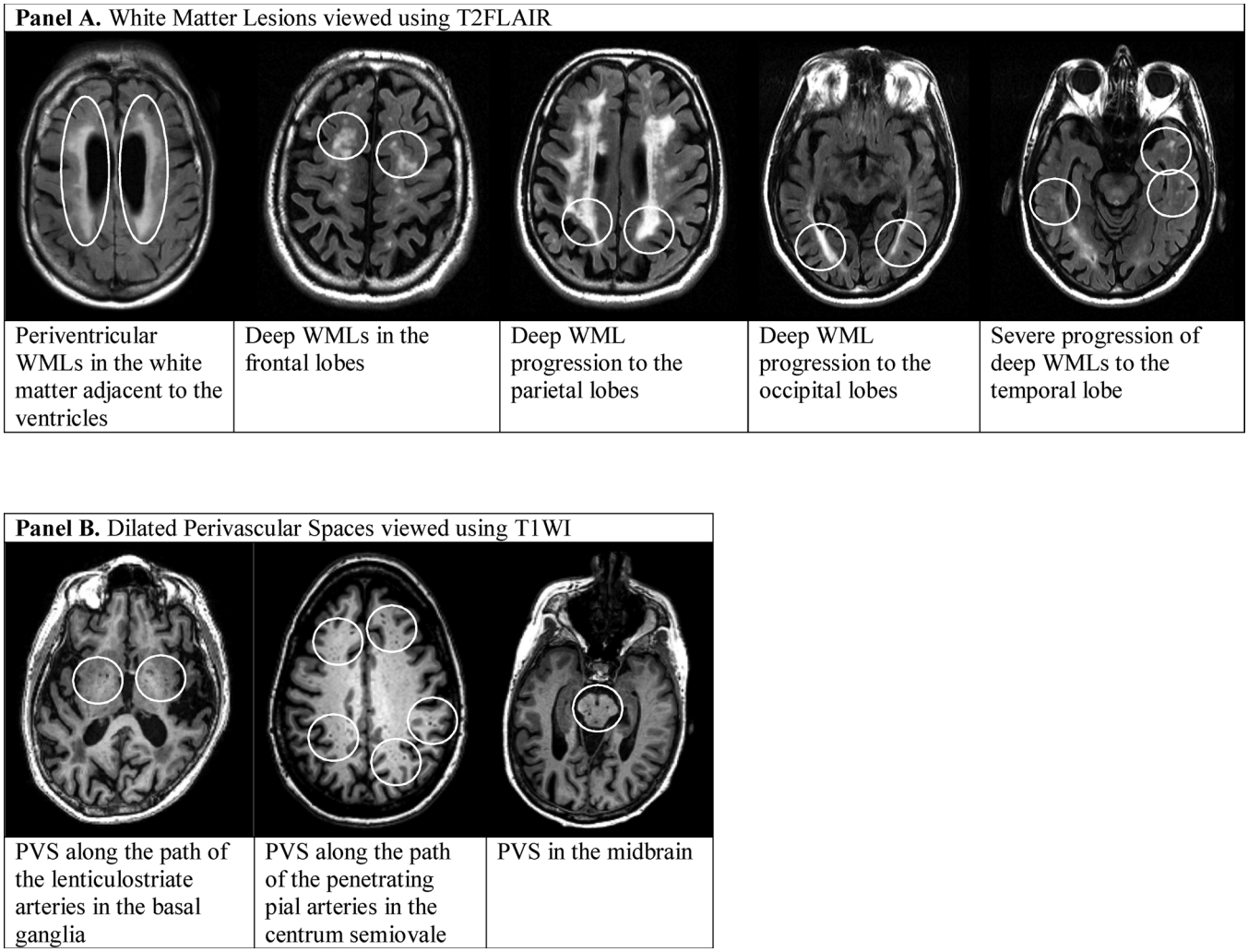

Fig. 3. Examples showing common locations of the periventricular and deep white matter lesions.

creation and validation of MRI based scales capable of assessing whole brain structural health in ageing will be an important endeavor.

These new methods of evaluating multiple changes simultaneously better reflect the nature of the systems we are assessing. The brain and body can be considered "complex systems", where high-level functions are the product of many subsystems, none of which could produce the function on their own, but which interact non-linearly to produce high-level effects (Cook, 2000). In this sense, high level functions of the brain and body can be considered emergent properties of their subsystems. These subsystems also include multiple interacting redundancies, and the capacity for active self-repair. In a simple system, failure of a single component often leads to system level failure, in contrast, complex systems fail through the accumulation of deficits which combine to overwhelm redundancies and repair abilities (Rockwood et al., 2017).

This understanding is somewhat intuitive. Brain functions are complex, and communication throughout interconnected networks is necessary for high level functions like cognition and memory. In consideration of how these functions fail with respect to the physiological changes discussed, we could imagine a case where a small change begins to affect the network, such as a lacune or PVS. At first, the small change alone would have little impact, as neurocompensatory effects act to maintain function. However, as the individual continues to age, additional neurodegenerative changes such as WMLs and microbleeds continue to degenerate the networks, and as atrophy proceeds, the amount of tissue will be reduced. Each change will further eliminate available redundancies and move the system closer to a failure state. Eventually, deficits throughout the network will accumulate to the point where the system will no longer be able to carry out its high level functions, and we will see cognitive decline or dementia. Thus, though these changes may appear to be small and occur in different parts of the system, it is their cumulative interactions that lead to failure.

With respect to this understanding, emerging whole brain assessment approaches demonstrate a clear advantage. Rather than conceptualizing the risk of high level system failure as the risk of contracting a single deficit that leads to failure, they consider how close the system is to failure in terms of deficits that accumulate to tax the systems' robustness and repair abilities (Zhang et al., 2011). Though some major systems contribute more to function, even smaller deficits, which might be considered benign in and of themselves, combine to tax the robustness of the system (Chen et al., 2010). This is supported by literature that links changes together, and finds the prediction of disease or degeneration can generally be improved by combining different age-related changes together for assessment (Zhang et al., 2012).

This method of holistic assessment of the degenerative process represents a cultural shift from some of the current ways we conceptualize age related neurodegeneration. Medical perspectives on neurodegenerative disorders necessitate diagnosis and categorization, but this may not accurately reflect the processes at play. While a medical professional needs to have a single diagnosis to move forward with treatment, this ignores the considerable heterogeneity in disease progression that occurs between individuals. This perspective can constrain our focus into looking for single underlying deficits that

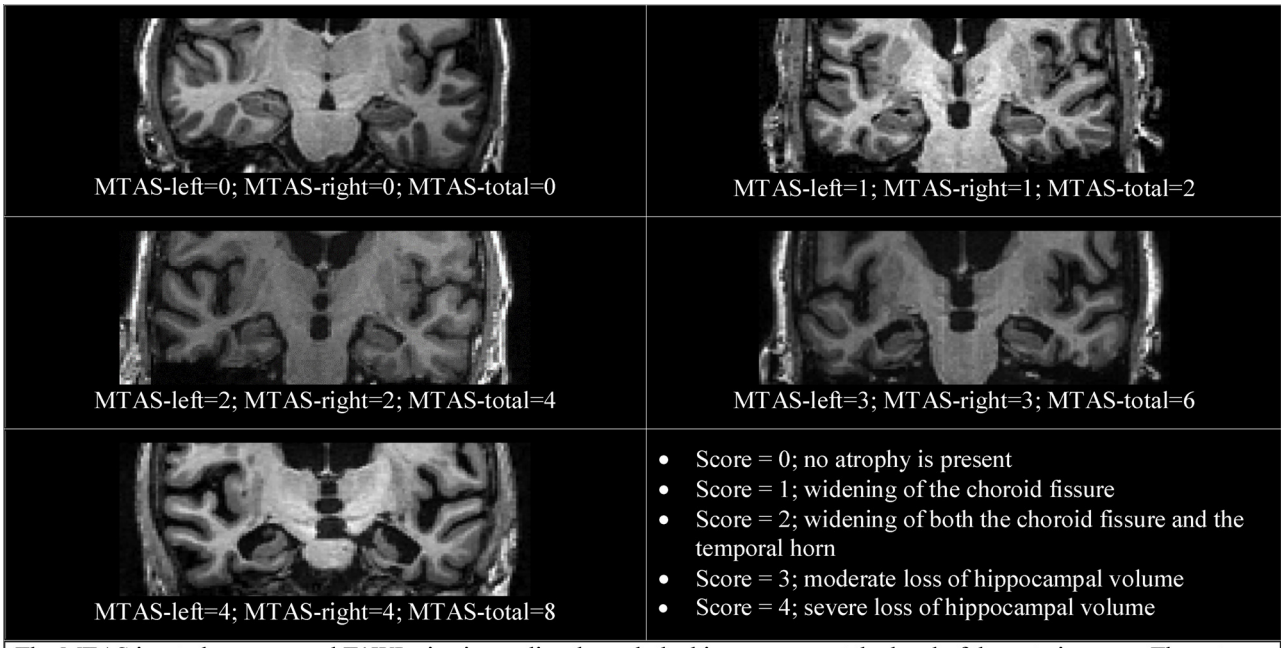

The MTAS is rated on a coronal T1WI, viewing a slice through the hippocampus at the level of the anterior pons. The rater will visually assess the width of the choroid fissure, the width of the temporal horn of the lateral ventricle, and the volume of the hippocampus itself. Based on the schema presented above, a score of 0 to 4 is assigned to score the atrophy level on the left and the right sides, with a large value indicating a more severe level of medial temporal lobe atrophy. Note the level of the atrophy can vary by side even in the same individual, although in these examples symmetrical medial temporal lobe atrophy patterns were observed, and thus the same scores were assigned. In patients 75 years of age or younger, a MTAS ≥ 2 (on either side) is considered as abnormal, whereas in patients 75 years of age or older, a MTAS ≥ 3 (on either side) is considered as abnormal. (Adapted from Scheltens et al. 1995)

Fig. 4. Examples showing evaluation of atrophy of the medial temporal lobes using the Medial Temporal Atrophy Scale (MTAS).

corresponds to a single diagnosis, when instead it may be prudent to think about multiple elements of degeneration interacting.

Given the importance assessing structural degeneration in the whole brain, MRI based rating systems are an ideal option. A system using structural MRI can simultaneously assess changes across the entire brain, and is easily accessible in research and clinical settings. Age related brain changes can be seen on MRI long before any cognitive symptoms appear (Frisoni et al., 2010), and can be even more sensitive than CSF markers and imaging markers of ABeta deposition (Jack et al., 2009; Sluimer et al., 2010). An MRI based index will also avoid more invasive tests, such as the painful spinal tap required to sample CSF, or exposure to ionizing radiation that occurs in a PET (Positron Emission Tomography) scan.

The accessibility of MRI in clinical settings is also imperative, as identifying neurodegeneration early will only increase in importance as our healthcare systems become increasingly burdened by the cost of dementia and age-related cognitive decline. Whole brain measures are also important as this cost does not just stem from major disorders like AD. There is considerable burden associated with non-specific age related cognitive impairment, such as the cost of nursing homes and healthcare, as well as the emotional burden and lost opportunity cost that comes from children caring for their elderly parents or family members.

Alongside its application in clinical environments, such a whole brain assessment tool would be useful in research settings and drug development. With a standardized method to assess and track neurodegeneration, researchers could apply the technique to large multicentre datasets to better understand how the whole brain changes with age and assess which risk factors and interventions are most significant. Importantly, the neurodegeneration seen on structural MRI has been shown to be modifiable (Mitnitski et al., 2013), with improvements in the health of the brain seen across various neurodegenerative changes. This gives hope that some interventions will be effective.

Possible next steps for developing whole brain neurodegeneration assessments would be to continue to validate them, to automate the image analysis, and to work to re-weight the algorithm that assesses the relative importance of each change. There are large datasets that track AD, and other disorders including CADASIL, but other dementias such as frontotemporal and vascular dementia do not have large neuroimaging datasets that would allow us to test the existing assessment tools. Broader neuroimaging datasets will assist with this push.

Overall, brain ageing is a process that occurs simultaneously across multiple domains, with different trajectories between individuals. As a complex system, the high-level failure in the brain occurs as a result of multiple insults that interact to overwhelm the repair capacities of the brain's subsystems. This means that even small neurodegenerative changes contribute to the additive effects of neurodegeneration, dementia, and cognitive impairment. We need to take this into account when we assess age related changes in the brain. A system that uses structural MRI is well suited to this purpose, and its development will have implications across clinical, research, and industry that will help us give our seniors lives worth living well into their twilight years.

Acknowledgements

We sincerely thank Ms. B. Chinda and Mrs. J. Grajauskas for proofreading the manuscript. We gratefully acknowledge Canadas National Science and Engineering Research Council (NSERC) for providing funding to L. Grajauskas; the China Scholarship Council for providing funding for H. Guo to conduct research in Canada; and the Canadian Institutes of Health Research (#CSE-125739) and Surrey Hospital and Outpatient Centre Foundation (#FHREB2015-030) for providing operating grants to X. Song.

References

Abbott, N.J., 2004. Evidence for bulk flow of brain interstitial fluid: significance for physiology and pathology. Neurochem. Int. 45 (4), 545–552.

Adams, H.H.H., Cavalieri, M., Verhaaren, B.F.J., Bos, D., van der Lugt, A., Enzinger, C., et al., 2013. Rating method for dilated Virchow–Robin spaces on magnetic resonance imaging. Stroke 44 (6) Retrieved from. http://stroke.ahajournals.org/content/44/6/1732.short.

Adams, H.H.H., Hilal, S., Schwingenschuh, P., Wittfeld, K., van der Lee, S.J., DeCarli, C., et al., 2015. A priori collaboration in population imaging: the uniform neuro-imaging of Virchow-robin spaces enlargement consortium. Alzheimer's Dement.: Diagn. Assess. Dis. Monit. 1 (4), 513–520. https://doi.org/10.1016/j.dadm.2015.10.004.

Alzheimer's Association, 2016. 2016 Alzheimer's Disease Facts and Figures, vol. 12 Alzheimer's & Dementia Elsevier.

Anderton, B.H., 2002. Ageing of the Brain. April 1. Mechanisms of Ageing and Development. Elsevierhttps://doi.org/10.1016/S0047-6374(01)00426-2.

Angulakshmi, M., Lakshmi Priya, G.G., 2017. Automated brain tumour segmentation techniques— a review. Int. J. Imaging Syst. Technol. 27 (1), 66–77. https://doi.org/10.1002/ima.22211.

Appel, J., Potter, E., Bhatia, N., Shen, Q., Zhao, W., Greig, M.T., et al., 2009. Association of white matter hyperintensity measurements on brain mr imaging with cognitive status, medial temporal atrophy, and cardiovascular risk factors. Am. J. Neuroradiol. https://doi.org/10.3174/ajnr.A1693.

Avants, B.B., Tustison, N.J., Song, G., Cook, P.A., Klein, A., Gee, J.C., 2011. A reproducible evaluation of ANTs similarity metric performance in brain image registration. Neuroimage 54 (3), 2033–2044.

Barber, R., Scheltens, P., Gholkar, A., Ballard, C., Mckeith, I., Ince, P., et al., 1999. White matter lesions on magnetic resonance imaging in dementia with Lewy bodies, Alzheimer's disease, vascular dementia, and normal aging. J. Neurol. Neurosurg. Psychiatry 67, 66–72. Retrieved from. https://www-ncbi-nlm-nih-gov.proxy.lib.sfu.ca/pmc/articles/PMC1736409/pdf/v067p00066.pdf.

Barkhof, F., 2004. Enlarged Virchow-Robin spaces: do they matter? J. Neurol. Neurosurg. Psychiatry 75 (11), 1516–1517.

Barnes, C.A., 2003. Long-term potentiation and the ageing brain. Philos. Trans. R. Soc. Lond. B Biol. Sci. 358 (1432), 765–772.

Boiten, J., Lodder, J., 1991. Lacunar infarcts. Pathogenesis and validity of the clinical syndromes. Stroke 22 (11), 1374–1378.

Bouvy, W.H., Biessels, G.J., Kuijf, H.J., Kappelle, L.J., Luijten, P.R., Zwanenburg, J.J.M., 2014. Visualization of perivascular spaces and perforating arteries with 7 T magnetic resonance imaging. Invest. Radiol. 49 (5), 307–313.

Boyle, P.A., Wilson, R.S., Yu, L., Barr, A.M., Honer, W.G., Schneider, J.A., Bennett, D.A., 2013. Much of late life cognitive decline is not due to common neurodegenerative pathologies. Ann. Neurol. 74 (3), 478–489. https://doi.org/10.1002/ana.23964.

Bracco, L., Piccini, C., Moretti, M., Mascalchi, M., Sforza, A., Nacmias, B., et al., 2005. Alzheimer's disease: role of size and location of white matter changes in determining cognitive deficits. Dement. Geriatr. Cogn. Disord. 20 (6), 358–366.

Breteler, M.M.B., Van Swieten, J.C., Bots, M.L., Grobbee, D.E., Claus, J.J., Van Den Hout, J.H.W., et al., 1994. Cerebral white matter lesions, vascular risk factors, and cognitive function in a population-based study: the Rotterdam Study. Neurology 44 (7), 1246.

Brickman, A.M., Honig, L.S., Scarmeas, N., Tatarina, O., Sanders, L., Albert, M.S., et al., 2008. Measuring cerebral atrophy and White Matter Hyperintensity Burden to predict the rate of cognitive decline in Alzheimer disease. Arch. Neurol. 65, 1202–1208.

Brickman, A.M., Provenzano, F.A., Muraskin, J., Manly, J.J., Blum, S., Apa, Z., et al., 2012. Regional white matter hyperintensity volume, not hippocampal atrophy, predicts incident Alzheimer disease in the community. Arch. Neurol. 69 (12), 1621–1627.

Brickman, A.M., Zahodne, L.B., Guzman, V.A., Narkhede, A., Meier, I.B., Griffith, E.Y., et al., 2015. Reconsidering harbingers of dementia: progression of parietal lobe white matter hyperintensities predicts Alzheimer's disease incidence. Neurobiol. Aging 36 (1), 27–32.

Briley, D.P., Wasay, M., Sergent, S., Thomas, S., 1997. Cerebral White Matter Changes (Leukoaraiosis), stroke, and gait disturbance. J. Am. Geriatr. Soc. 45 (12), 1434–1438. https://doi.org/10.1111/j.1532-5415.1997.tb03192.x.

Brundel, M., De Bresser, J., Van Dillen, J.J., Kappelle, L.J., Biessels, G.J., 2012. Cerebral microinfarcts: a systematic review of neuropathological studies. J. Cereb. Blood Flow Metab. 32 (3), 425–436. https://doi.org/10.1038/jcbfm.2011.200.

Caligiuri, M.E., Perrotta, P., Augimeri, A., Rocca, F., Quattrone, A., Cherubini, A., 2015. Automatic detection of white matter hyperintensities in healthy aging and pathology using magnetic resonance imaging: a review. Neuroinformatics 13 (3), 261–276. https://doi.org/10.1007/s12021-015-9260-y.

Caplan, L.R., 2015. Lacunar infarction and small vessel disease: pathology and pathophysiology. J. Stroke 17 (1), 2–6. https://doi.org/10.5853/jos.2015.17.1.2.

Cees De Groot, J., De Leeuw, F., Oudkerk, M., Van Gijn, J., Hofman, A., Jolles, J., Breteler, M., 2000. Cerebral white matter lesions and cognitive function: the Rotterdam scan Study. Ann. Neurol. 47 (2), 145–151.

Chabriat, H., Joutel, A., Dichgans, M., Tournier-Lasserve, E., Bousser, M.-G., 2009. Cadasil. Lancet Neurol. 8 (7), 643–653.

Chen, W., Song, X., Zhang, Y., Darvesh, S., Zhang, N., D'Arcy, R.C.N., et al., 2010. An MRI-based semiquantitative index for the evaluation of brain atrophy and lesions in Alzheimer's disease, mild cognitive impairment and normal aging. Dement. Geriatr. Cognit. Disord. 30 (2), 121–130. https://doi.org/10.1159/000319537.

Chen, W., Song, X., Zhang, Y., 2011. Assessment of the virchow-robin spaces in Alzheimer disease, mild cognitive impairment, and normal aging, using high-field MR imaging. Am. J. Neuroradiol. 32 (8), 1490–1495. https://doi.org/10.3174/ajnr.A2541.

Chowdhury, M.H., Nagai, A., Bokura, H., Nakamura, E., Kobayashi, S., Yamaguchi, S., 2011. Age-related changes in white matter lesions, hippocampal atrophy, and cerebral microbleeds in healthy subjects without major cerebrovascular risk factors. J. Stroke Cerebrovasc. Dis. 20, 302–309. https://doi.org/10.1016/j.jstrokecerebrovasdis.2009.12.010.

Cointepas, Y., Mangin, J.-F., Garnero, L., Poline, J.-B., Benali, H., 2001. BrainVISA: software platform for visualization and analysis of multi-modality brain data. Neuroimage 13 (6), 98.

Cole, J.H., Franke, K., 2017. Predicting age using neuroimaging: innovative brain ageing biomarkers. Trends Neurosci. 40 (12), 681–690. https://doi.org/10.1016/j.tins.2017.10.001.

Cook, R.I., 2000. How Complex Systems Fail. Retrieved from. Cognitive Technologies Laboratory; University of Chicago, pp. 1–5. http://web.mit.edu/2.75/resources/random/HowComplexSystemsFail.pdf.

Craddock, R.C., Bellec, P., Jbabdi, S., 2017. Neuroimage special issue on brain segmentation and parcellation - editorial. NeuroImage 5–8. https://doi.org/10.1016/j.neuroimage.2017.11.063.

Cumurciuc, R., Guichard, J., Reizine, D., Gray, F., Bousser, M.G., Chabriat, H., 2006. Dilation of Virchow-Robin spaces in CADASIL. Eur. J. Neurol. 13 (2), 187–190.

Davies, R.R., Kipps, C.M., Mitchell, J., Kril, J.J., Halliday, G.M., Hodges, J.R., 2006. Progression in frontotemporal dementia: identifying a benign behavioral variant by magnetic resonance imaging. Arch. Neurol. 63 (11), 1627–1631.

DeCarli, C., Miller, B.L., Swan, G.E., Reed, T., Wolf, P.A., Garner, J., et al., 1999. Predictors of brain morphology for the men of the NHLBI twin study. Stroke 30 (3), 529–536. https://doi.org/10.1161/01.STR.30.3.529.

Ding, J., Sigurðsson, S., Jónsson, P.V., Eiriksdottir, G., Charidimou, A., Lopez, O.L., et al., 2017a. Large perivascular spaces visible on magnetic resonance imaging, cerebral small vessel disease progression, and risk of dementia. JAMA Neurol. 74 (9), 1105. https://doi.org/10.1001/jamaneurol.2017.1397.

Ding, Z., Huang, Y., Bailey, S.K., Gao, Y., Cutting, L.E., Rogers, B.P., 2017b. Detection of Synchronous Brain Activity in White Matter Tracts at Rest and Under Functional Loading. pp. 1–6. https://doi.org/10.1073/pnas.1711567115.

Double, K.L., Halliday, G.M., Krill, J.J., Harasty, J.A., Cullen, K., Brooks, W.S., Creasey, H., Broe, G.A., 1996. Topography of brain atrophy during normal aging and Alzheimer's disease. Neurobiol. Aging 17 (4), 513–521. https://doi.org/10.1016/0197-4580(96)00005-X.

Duchesnay, E., Selem, F.H., De Guio, F., Dubois, M., Mangin, J.F., Duering, M., et al., 2018. Different types of white matter hyperintensities in CADASIL. Front. Neurol. 9 (July), 1–8. https://doi.org/10.3389/fneur.2018.00526.

Enzinger, C., Fazekas, F., Matthews, P.M., Ropele, S., Schmidt, H., Smith, S., Schmidt, R., 2005. Risk factors for progression of brain atrophy in aging: six-year follow-up of normal subjects. Neurology 64 (10), 1704–1711. https://doi.org/10.1212/01.WNL.0000161871.83614.BB.

Favaretto, A., Lazzarotto, A., Riccardi, A., Pravato, S., Margoni, M., Causin, F., et al., 2017. Enlarged Virchow Robin spaces associate with cognitive decline in multiple sclerosis. PLoS One 12 (10). https://doi.org/10.1371/journal.pone.0185626.e0185626.

Fazekas, F., Chawluk, J.B., Alavi, A., Hurtig, H.I., Zimmerman, R.A., 1987. Mr signal abnormalities at 1.5-T in Alzheimer dementia and normal aging. Am. J. Roentgenol. 149 (2), 351–356. https://doi.org/10.2214/ajr.149.2.351.

Fazekas, F., Kleinert, R., Offenbacher, H., Schmidt, R., Kleinert, G., Payer, F., et al., 1993. Pathologic correlates of incidental MRI white matter signal hyperintensities. Neurology 43 (9), 1683–1689. https://doi.org/10.1212/WNL.43.9.1683.

Fazekas, F., Kleinert, R., Roob, G., Kleinert, G., Kapeller, P., Schmidt, R., Hartung, H.-P., 1999. Histopathologic analysis of foci of signal loss on gradient-echo T2*-weighted MR images in patients with spontaneous intracerebral hemorrhage: evidence of microangiopathy-related microbleeds. Am. J. Neuroradiol. 20 (4), 637–642.

Fedorov, A., Beichel, R., Kalpathy-Cramer, J., Finet, J., Fillion-Robin, J.-C., Pujol, S., et al., 2012. 3D Slicer as an image computing platform for the quantitative imaging network. Mag. Reson. Imaging 30 (9), 1323–1341.

Ferreira, D., Verhagen, C., Hernández-Cabrera, J.A., Cavallin, L., Guo, C.J., Ekman, U., et al., 2017. Distinct subtypes of Alzheimer's disease based on patterns of brain atrophy: longitudinal trajectories and clinical applications. Sci. Rep. 7 (April), 1–13. https://doi.org/10.1038/srep46263.

Fischl, B., 2012. FreeSurfer. Neuroimage 62 (2), 774–781.

Fjell, A.M., 2010. Structural brain changes in aging: courses, causes and cognitive consequences. Rev. Neurosci. 21 (3), 187–221. https://doi.org/10.1515/REVNEURO.2010.21.3.187.

Frisoni, G.B., Fox, N.C., Jack, C.R., Scheltens, P., Thompson, P.M., 2010. The clinical use of structural MRI in Alzheimer disease. Nat. Rev. Neurol. https://doi.org/10.1038/nrneurol.2009.215.

Galluzzi, S., Lanni, C., Pantoni, L., Filippi, M., Frisoni, G.B., 2008. White matter lesions in the elderly: pathophysiological hypothesis on the effect on brain plasticity and reserve. J. Neurol. Sci. 273 (1–2), 3–9. https://doi.org/10.1016/j.jns.2008.06.023.

Godin, O., Dufouil, C., Maillard, P., Delcroix, N., Mazoyer, B., Crivello, F., et al., 2008. White matter lesions as a predictor of depression in the elderly: the 3C-Dijon study. Biol. Psychiatry 63 (7), 663–669. https://doi.org/10.1016/j.biopsych.2007.09.006.

Goldstein, I.B., Bartzokis, G., Guthrie, D., Shapiro, D., 2002. Ambulatory blood pressure and brain atrophy in the healthy elderly. Neurology 59 (5), 713–719. https://doi.org/10.1212/WNL.59.5.713.

Gouw, A.A., Van der Flier, W.M., Van Straaten, E.C.W., Barkhof, F., Ferro, J.M., Baezner, H., et al., 2006. Simple versus complex assessment of white matter hyperintensities in relation to physical performance and cognition: the LADIS study. J. Neurol. 253 (9), 1189.

Grajauskas, L.A., Guo, H., D'Arcy, R.C.N., Song, X., 2018. Toward MRI-based whole-brain health assessment: the brain atrophy and lesion index (BALI). Aging Med. 1 (1), 55–63.

Greenberg, S.M., Eng, J.A., Ning, M., Smith, E.E., Rosand, J., 2004. Hemorrhage burden predicts recurrent intracerebral hemorrhage after lobar hemorrhage. Stroke 35 (6), 1415–1420.
Greenberg, S.M., Vernooij, M.W., Cordonnier, C., Viswanathan, A., Al-Shahi Salman, R., Warach, S., et al., 2009. Cerebral microbleeds: a guide to detection and interpretation. Lancet Neurol. 8 (2), 165–174. https://doi.org/10.1016/S1474-4422(09)70013-4.
Griffanti, L., Zamboni, G., Khan, A., Li, L., Bonifacio, G., Sundaresan, V., et al., 2016. BIANCA (Brain Intensity AbNormality Classification Algorithm): a new tool for automated segmentation of white matter hyperintensities. NeuroImage 141, 191–205. https://doi.org/10.1016/j.neuroimage.2016.07.018.
Groeschel, S., Chong, W.K., Surtees, R., Hanefeld, F., 2006. Virchow-Robin spaces on magnetic resonance images: normative data, their dilatation, and a review of the literature. Neuroradiology 48 (10), 745–754. https://doi.org/10.1007/s00234-006-0112-1.
Grueter, B.E., Schulz, U.G., 2012. Age-related cerebral white matter disease (leukoaraiosis): a review. Postgrad. Med. J. 88 (1036), 79–87. https://doi.org/10.1136/postgradmedj-2011-130307.
Guo, H., Song, X., Schmidt, M.H., Vandorpe, R., Yang, Z., LeBlanc, E., et al., 2014a. Evaluation of whole brain health in aging and Alzheimer's disease: a standard procedure for scoring an MRI-based brain atrophy and lesion index. J. Alzheimer's Dis. https://doi.org/10.3233/JAD-140333.
Guo, H., Song, X., Vandorpe, R., Zhang, Y., Chen, W., Zhang, N., et al., 2014b. Evaluation of common structural brain changes in aging and Alzheimer disease with the use of an MRI-based brain atrophy and lesion index: a comparison between T1WI and T2WI at 1.5T and 3T. Am. J. Neuroradiol. https://doi.org/10.3174/ajnr.A3709.
Guo, H., Siu, W., D'Arcy, R.C., Black, S.E., Grajauskas, L.A., Singh, S., et al., 2017. MRI assessment of whole-brain structural changes in aging. Clin. Intervent. Aging 12, 1251–1270. https://doi.org/10.2147/CIA.S139515.
Haglund, M., Passant, U., Sjöbeck, M., Ghebremedhin, E., Englund, E., 2006. Cerebral amyloid angiopathy and cortical microinfarcts as putative substrates of vascular dementia. Int. J. Geriatr. Psychiatry 21 (7), 681–687. https://doi.org/10.1002/gps.1550.
Harper, L., Fumagalli, G.G., Barkhof, F., Scheltens, P., O'Brien, J.T., Bouwman, F., et al., 2016. MRI visual rating scales in the diagnosis of dementia: evaluation in 184 post-mortem confirmed cases. Brain: J. Neurol. 139 (Pt 4), 1211–1225. https://doi.org/10.1093/brain/aww005.
Harteveld, A.A., van der Kolk, A.G., Zwanenburg, J.J.M., Luijten, P.R., Hendrikse, J., 2016. 7-T MRI in cerebrovascular diseases: challenges to overcome and initial results. Top. Mag. Reson. Imaging 25 (2), 89–100.
Hedman, A.M., van Haren, N.E.M., Schnack, H.G., Kahn, R.S., Hulshoff Pol, H.E., 2012. Human brain changes across the life span: a review of 56 longitudinal magnetic resonance imaging studies. Human Brain Mapp. 33 (8), 1987–2002. https://doi.org/10.1002/hbm.21334.
Hernández, M.C.V., Piper, R.J., Wang, X., Deary, I.J., Wardlaw, J.M., Hernandez, M., et al., 2013. Towards the automatic computational assessment of enlarged perivascular spaces on brain magnetic resonance images: a systematic review. J. Mag. Reson. Imaging 38 (4), 774–785. https://doi.org/10.1002/jmri.24047.
Homeyer, P., Cornu, P., Lacomblez, L., Chiras, J., Derouesne, C., 1996. A special form of cerebral lacunae: expanding lacunae. J. Neurol. Neurosurg. Psychiatry 61 (2), 200–202.
Hopkins, R.O., Beck, C.J., Burnett, D.L., Weaver, L.K., Victoroff, J., Bigler, E.D., 2006. Prevalence of white matter hyperintensities in a young healthy population. J. Neuroimaging 16 (3), 243–251.
Howard, R., Cox, T., Almeida, O., Mullen, R., Graves, P., Reveley, A., Levy, R., 1995. White matter signal hyperintensities in the brains of patients with late paraphrenia and the normal, community-living elderly. Biol. Psychiatry 38 (2), 86–91. https://doi.org/10.1016/0006-3223(94)00248-2.
Hurford, R., Charidimou, A., Fox, Z., Cipolotti, L., Jager, R., Werring, D.J., 2014. MRI-visible perivascular spaces: relationship to cognition and small vessel disease MRI markers in ischaemic stroke and TIA. J. Neurol. Neurosurg. Psychiatry 85 (5), 522–525. https://doi.org/10.1136/jnnp-2013-305815.
Iturria-Medina, Y., Sotero, R.C., Toussaint, P.J., Mateos-Pérez, J.M., Evans, A.C., Weiner, M.W., et al., 2016. Early role of vascular dysregulation on late-onset Alzheimer's disease based on multifactorial data-driven analysis. Nat. Commun. 7, 11934. https://doi.org/10.1038/ncomms11934.
Jack, C.R., Lowe, V.J., Weigand, S.D., Wiste, H.J., Senjem, M.L., Knopman, D.S., et al., 2009. Serial PIB and MRI in normal, mild cognitive impairment and Alzheimer's disease: implications for sequence of pathological events in Alzheimer's disease. Brain 132 (5), 1355–1365. https://doi.org/10.1093/brain/awp062.
Jacobs, H.I.L.L., Van Boxtel, M.P.J., Van Der Elst, W., Burgmans, S., Smeets, F., Gronenschild, E.H.B.M.B.M., et al., 2011. Increasing the diagnostic accuracy of medial temporal lobe atrophy in alzheimer's disease. J. Alzheimer's Dis. 25 (3), 477–490. https://doi.org/10.3233/JAD-2011-102043.
Jang, J.-W., Park, S.Y., Park, Y.H., Baek, M.J., Lim, J.-S., Youn, Y.C., Kim, S., 2015. A comprehensive visual rating scale of brain magnetic resonance imaging: application in elderly subjects with Alzheimer's disease, mild cognitive impairment, and normal cognition. J. Alzheimer's Dis. 44 (3), 1023–1034. https://doi.org/10.3233/JAD-142088.
Jiang, J., Sachdev, P., Lipnicki, D.M., Zhang, H., Liu, T., Zhu, W., et al., 2014. A longitudinal study of brain atrophy over two years in community-dwelling older individuals. NeuroImage. https://doi.org/10.1016/j.neuroimage.2013.08.022.
Joutel, A., Corpechot, C., Ducros, A., Vahedi, K., Chabriat, H., Mouton, P., et al., 1996. Notch3 mutations in CADASIL, a hereditary adult-onset condition causing stroke and dementia. Nature 383 (6602), 707.
Jungreis, C.A., Kanal, E., Hirsch, W.L., Martinez, A.J., Moossy, J., 1988. Normal perivascular spaces mimicking lacunar infarction: MR imaging. Radiology 169 (1), 101–104.
Kalmijn, S., Foley, D., White, L., Burchfiel, C.M., Curb, J.D., Petrovitch, H., et al., 2000. Metabolic cardiovascular syndrome and risk of dementia in Japanese-American elderly men. The Honolulu-Asia aging study. Arterioscler. Thromb. Vasc. Biol. 20 (10), 2255–2260. https://doi.org/10.1161/01.ATV.20.10.2255.
Keller, S.S., Roberts, N., 2009. Measurement of brain volume using MRI: software, techniques, choices and prerequisites. J. Anthropol. Sci. 87, 127–151.
Kim, K.W., MacFall, J.R., Payne, M.E., 2008. Classification of white matter lesions on magnetic resonance imaging in elderly persons. Biol. Psychiatry 64 (4), 273–280.
Kipps, C.M., Davies, R.R., Mitchell, J., Kril, J.J., Halliday, G.M., Hodges, J.R., 2007. Clinical significance of lobar atrophy in frontotemporal dementia: application of an MRI visual rating scale. Dement. Geriatr. Cognit. Disord. 23 (5), 334–342.
Knudsen, K.A., Rosand, J., Karluk, D., Greenberg, S.M., 2001. Clinical diagnosis of cerebral amyloid angiopathy: validation of the Boston criteria. Neurology 56 (4), 537–539.
Koedam, E.L.G.E., Lehmann, M., van der Flier, W.M., Scheltens, P., Pijnenburg, Y.A.L., Fox, N., et al., 2011. Visual assessment of posterior atrophy development of a MRI rating scale. Eur. Radiol. 21 (12), 2618–2625.
Kuo, H.-K., Lipsitz, L.A., 2004. Cerebral white matter changes and geriatric syndromes: is there a link? J. Gerontol. Ser. A: Biol. Sci. Med. Sci. 59 (8), M818–M826. https://doi.org/10.1093/gerona/59.8.M818.
Kwee, R.M., Kwee, T.C., 2007. Virchow-robin spaces at MR imaging. RadioGraphics 27 (4), 1071–1086. https://doi.org/10.1148/rg.274065722.
Lammie, G.A., 2000. Pathology of small vessel stroke. Br. Med. Bull. 56 (2), 296–306. https://doi.org/10.1258/0007142001903229.
Lampe, L., Kharabian-Masouleh, S., Kynast, J., Arelin, K., Steele, C.J., Löffler, M., et al., 2017. Lesion location matters: the relationships between white matter hyperintensities on cognition in the healthy elderly. J. Cereb. Blood Flow Metab. https://doi.org/10.1177/0271678X17740501.
Launer, L.J., Berger, K., Breteler, M.M.B., Dufouil, C., Fuhrer, R., Giampaoli, S., et al., 2006. Regional variability in the prevalence of cerebral white matter lesions: an MRI study in 9 European countries (CASCADE). Neuroepidemiology 26 (1), 23–29.
Leys, D., Englund, E., Del Ser, T., Inzitari, D., Fazekas, F., Bornstein, N., et al., 1999. White matter changes in stroke patients. Relationship with stroke subtype and outcome. Eur. Neurol. 42 (2), 67–75. https://doi.org/69414.
Li, F., Takechi, H., Saito, R., Ayaki, T., Kokuryu, A., Kuzuya, A., Takahashi, R., 2018. A comparative study: visual rating scores and the voxel-based specific regional analysis system for Alzheimer's disease on magnetic resonance imaging among subjects with Alzheimer's disease, mild cognitive impairment, and normal cognition. Psychogeriatrics.
Lindemer, E.R., Salat, D.H., Smith, E.E., Nguyen, K., Fischl, B., Greve, D.N., 2015. White matter signal abnormality quality differentiates mild cognitive impairment that converts to Alzheimer's disease from nonconverters. Neurobiol. Aging 36 (9), 2447–2457.
Longstreth, W.T.T., Manolio, T.A., Arnold, A., Burke, G.L., Bryan, N., Jungreis, C.A., et al., 1996. Clinical correlates of white matter findings on cranial magnetic resonance imaging of 3301 elderly people: the Cardiovascular Health Study. Stroke 27 (8), 1274–1282. Retrieved from. http://www.ncbi.nlm.nih.gov/pubmed/8711786.
Longstreth, W.T., Arnold, A.M., Manolio, T.A., Burke, G.L., Bryan, N., Jungreis, C.A., et al., 2000. Clinical correlates of ventricular and sulcal size on cranial magnetic resonance imaging of 3,301 elderly people. Neuroepidemiology 19 (1), 30–42.
Maclullich, A.M.J., Wardlaw, J.M., Ferguson, K.J., Starr, J.M., Seckl, J.R., Deary, I.J., 2004. Enlarged perivascular spaces are associated with cognitive function in healthy elderly men. J. Neurol. Neurosurg. Psychiatry 75, 1519–1523. https://doi.org/10.1136/jnnp.2003.030858.
Mitnitski, A., Song, X., Rockwood, K., 2013. Assessing biological aging: the origin of deficit accumulation. Biogerontology 14 (6), 709–717. https://doi.org/10.1007/s10522-013-9446-3.
Miyata, M., Kakeda, S., Iwata, S., Nakayamada, S., Ide, S., Watanabe, K., et al., 2017. Enlarged perivascular spaces are associated with the disease activity in systemic lupus erythematosus. Sci. Rep. 7 (1), 12566. https://doi.org/10.1038/s41598-017-12966-4.
O'Brien, J., Desmond, P., Ames, D., Schweitzer, I., Harrigan, S., Tress, B., 1996. A magnetic resonance imaging study of white matter lesions in depression and Alzheimer's disease. Br. J. Psychiatry: J. Ment. Sci. 168 (4), 477–485. https://doi.org/10.1192/BJP.168.4.477.
Oberstein, S.A.J.L., Van den Boom, R., Van Buchem, M.A., Van Houwelingen, H.C., Bakker, E., Vollebregt, E., et al., 2001. Cerebral microbleeds in CADASIL. Neurology 57 (6), 1066–1070.
Oster, S., Christoffersen, Per Gundersen, H.G., Nielsen, J.O., Pedersen, C., Pakkenberg, R., 1995. Six Billion Neurons Lost in AIDS: a Stereological Study of the Neocortex. March 1. APMIS. Blackwell Publishing Ltdhttps://doi.org/10.1111/j.1699-0463.1995.tb01401.x.
Pakkenberg, B., Pelvig, D., Marner, L., Bundgaard, M.J., Gundersen, H.J.G., Nyengaard, J.R., Regeur, L., 2003. Aging and the human neocortex. Experimental Gerontology, vol. 38 Pergamonhttps://doi.org/10.1016/S0531-5565(02)00151-1. pp. 95–99.
Pantoni, L., 2010. Cerebral small vessel disease: from pathogenesis and clinical characteristics to therapeutic challenges. Lancet Neurol. 9 (7), 689–701. https://doi.org/10.1016/S1474-4422(10)70104-6.
Pantoni, L., Simoni, M., Pracucci, G., Schmidt, R., Barkhof, F., Inzitari, D., 2002. Visual rating scales for age-related white matter changes (leukoaraiosis): can the heterogeneity be reduced? Stroke 33 (12), 2827–2833.
Park, J.B., 2014. Hypertensive vasculopathy. Pulse 2 (1–4), 38–41.
Park, M., Moon, W.-J., 2016. Structural MR imaging in the diagnosis of alzheimer's disease and other neurodegenerative dementia: current imaging approach and future

perspectives. Korean J. Radiol. 17 (6), 827–845.
Pasquier, F., Leys, D., Weerts, J.G.E.E., Mounier-Vehier, F., Barkhof, F., Scheltens, P., 1996. Inter-and intraobserver reproducibility of cerebral atrophy assessment on MRI scans with hemispheric infarcts. Eur. Neurol. 36 (5), 268–272. https://doi.org/10.1159/000117270.
Patankar, T.F., Mitra, D., Varma, A., Snowden, J., Neary, D., Jackson, A., 2005. Dilatation of the Virchow-Robin space is a sensitive indicator of cerebral microvascular disease: study in elderly patients with dementia. Am. J. Neuroradiol. 26 (6), 1512–1520. Retrieved from. http://www.ajnr.org/content/ajnr/26/6/1512.full.pdf.
Peters, R., 2006. Ageing and the brain. Postgrad. Med. J. 82 (964), 84–88. https://doi.org/10.1136/pgmj.2005.036665.
Peters, A., Morrison, J.H., Rosene, D.L., Hyman, B.T., 1998. Feature article are neurons lost from the primate cerebral cortex during normal aging? Cereb. Cortex. https://doi.org/10.1093/cercor/8.4.295.
Pini, L., Pievani, M., Bocchetta, M., Altomare, D., Bosco, P., Cavedo, E., et al., 2016. Brain atrophy in Alzheimer's disease and aging. Ageing Res. Rev. 30, 25–48. https://doi.org/10.1016/j.arr.2016.01.002.
Potter, G.M., Chappell, F.M., Morris, Z., Wardlaw, J.M., 2015a. Cerebral perivascular spaces visible on magnetic resonance imaging: development of a qualitative rating scale and its observer reliability. Cerebrovasc. Dis. 39 (3–4), 224–231. https://doi.org/10.1159/000375153.
Potter, G.M., Doubal, F.N., Jackson, C.A., Chappell, F.M., Sudlow, C.L., Dennis, M.S., Wardlaw, J.M., 2015b. Enlarged perivascular spaces and cerebral small vessel disease. Int. J. Stroke 10 (3), 376–381. https://doi.org/10.1111/ijs.12054.
Prasad, K., Wiryasaputra, L., Ng, A., Kandiah, N., 2011. White matter disease independently predicts progression from mild cognitive impairment to alzheimer's disease in a clinic cohort. Dement. Geriatr. Cognit. Disord. 31 (6), 431–434. https://doi.org/10.1159/000330019.
Prince, M., Bryce, R., Albanese, E., Wimo, A., Ribeiro, W., Ferri, C.P., 2013. The global prevalence of dementia: a systematic review and metaanalysis. Alzheimer's Dement.: J. Alzheimer's Assoc. 9 (1), 63–75.
Prins, N.D., van Straaten, E.C.W., van Dijk, E.J., Simoni, M., van Schijndel, R.A., Vrooman, H.A., et al., 2004. Measuring progression of cerebral white matter lesions on MRI: visual rating and volumetrics. Neurology 62 (9), 1533–1539. https://doi.org/10.1212/01.WNL.0000123264.40498.B6.
Ramirez, J., Berezuk, C., McNeely, A.A., Scott, C.J.M., Gao, F., Black, S.E., 2015. Visible Virchow-Robin spaces on magnetic resonance imaging of Alzheimer's disease patients and normal elderly from the Sunnybrook dementia study. J. Alzheimer's Dis. 43 (2), 415–424. https://doi.org/10.3233/JAD-132528.
Ramirez, J., Berezuk, C., McNeely, A.A., Gao, F., McLaurin, J.A., Black, S.E., 2016. Imaging the perivascular space as a potential biomarker of neurovascular and neurodegenerative diseases. Cell. Mol. Neurobiol. 36 (2), 289–299. https://doi.org/10.1007/s10571-016-0343-6.
Ramji, S., Touska, P., Rich, P., Mackinnon, A.D., 2017. Normal neuroanatomical variants that may be misinterpreted as disease entities. Clin. Radiol. 72 (10), 810–825. Retrieved from. http://www.sciencedirect.com.proxy.lib.sfu.ca/science/article/pii/S0009926017303483?via%3Dihub#.
Raz, N., 2004. The aging brain: structural changes and their implications for cognitive aging. New Front. Cognit. Aging 115–133.
Raz, N., Ghisletta, P., Rodrigue, K.M., Kennedy, K.M., Lindenberger, U., 2010. Trajectories of brain aging in middle-aged and older adults: regional and individual differences. NeuroImage 51 (2), 501–511. https://doi.org/10.1016/J.NEUROIMAGE.2010.03.020.
Regeur, L., Jensen, G.B., Pakkenberg, H., Evans, S.M., Pakkenberg, B., 1994. No global neocortical nerve cell loss in brains from patients with senile dementia of Alzheimer's type. Neurobiol. Aging 15 (3), 197–4580. Retrieved from. https://ac-els-cdn-com.proxy.lib.sfu.ca/0197458094900302/1-s2.0-0197458094900302-main.pdf?_tid=9db343b4-f285-11e7-a060-00000aab0f27&acdnat=1515204315_e83713f5c76cf761cefd5c4d847f0e88.
Rockwood, K., Mitnitski, A., 2011. Frailty defined by deficit accumulation and geriatric medicine defined by frailty. Clin. Geriatr. Med. 27 (1), 17–26.
Rockwood, K., Blodgett, J.M., Theou, O., Sun, M.H., Feridooni, H.A., Mitnitski, A., et al., 2017. A frailty index based on deficit accumulation quantifies mortality risk in humans and in mice. Sci. Rep. 7, 43068. https://doi.org/10.1038/srep43068.
Rosenberg, G.A., Sullivan, N., Esiri, M.M., 2001. White matter damage is associated with matrix metalloproteinases in vascular dementia. Stroke 32 (5), 1162–1168. https://doi.org/10.1161/01.STR.32.5.1162.
Sakakibara, R., Hattori, T., Uchiyama, T., Yamanishi, T., 1999. Urinary function in elderly people with and without leukoaraiosis: relation to cognitive and gait function. J. Neurol. Neurosurg. Psychiatry 67 (5), 658–660. https://doi.org/10.1136/JNNP.67.5.658.
Satizabal, C.L., Zhu, Y.-C., Dufouil, C., Tzourio, C., 2013. Inflammatory proteins and the severity of dilated Virchow-Robin spaces in the elderly. J. Alzheimer's Dis. 33 (2), 323–328.
Scheltens, P., Barkhof, F., Leys, D., Pruvo, J.P., Nauta, J.J.P.J.P., Vermersch, P., et al., 1993. A semiquantative rating scale for the assessment of signal hyperintensities on magnetic resonance imaging. J. Neurol. Sci. 114 (1), 7–12. https://doi.org/10.1016/0022-510X(93)90041-V.
Scheltens, P., Launer, L.J., Barkhof, F., Weinstein, H.C., Van Gool, W.A., Scheltens, P., et al., 1995. Visual assessment of medial temporal lobe atrophy on magnetic resonance imaging: interobserver reliability. J. Neurol. 242, 557–560. Retrieved from. https://link-springer-com.proxy.lib.sfu.ca/content/pdf/10.1007%2FBF00868807.pdf.
Schley, D., Carare-Nnadi, R., Please, C.P., Perry, V.H., Weller, R.O., 2006. Mechanisms to explain the reverse perivascular transport of solutes out of the brain. J. Theor. Biol. 238 (4), 962–974. https://doi.org/10.1016/j.jtbi.2005.07.005.
Schmidt, R., Ropele, S., Enzinger, C., Petrovic, K., Smith, S., Schmidt, H., et al., 2005. White matter lesion progression, brain atrophy, and cognitive decline: the Austrian stroke prevention study. Ann. Neurol. 58 (4), 610–616. https://doi.org/10.1002/ana.20630.
Schuff, N., Tosun, D., Insel, P.S., Chiang, G.C., Truran, D., Aisen, P.S., et al., 2012. Nonlinear time course of brain volume loss in cognitively normal and impaired elders. Neurobiol. Aging 33 (5), 845–855.
Shi, Y., Wardlaw, J.M., 2016. Update on cerebral small vessel disease: a dynamic whole-brain disease. BMJ 1 (3), 83–92. https://doi.org/10.1136/svn-2016-000035.
Shiratori, K., Mrowka, M., Toussaint, A., Spalke, G., Bien, S., 2002. Extreme, unilateral widening of Virchow-Robin spaces: case report. Neuroradiology 44 (12), 990–992. https://doi.org/10.1007/s00234-002-0840-9.
Sigurdsson, S., Aspelund, T., Forsberg, L., Fredriksson, J., Kjartansson, O., Oskarsdottir, B., et al., 2012. Brain tissue volumes in the general population of the elderly. The AGES-Reykjavik study. NeuroImage 59 (4), 3862–3870. https://doi.org/10.1016/j.neuroimage.2011.11.024.
Sluimer, J.D., Bouwman, F.H., Vrenken, H., Blankenstein, M.A., Barkhof, F., Van Der Flier, W.M., Scheltens, P., 2010. Whole-brain atrophy rate and CSF biomarker levels in MCI and AD: a longitudinal study. Neurobiol. Aging 31, 758–764. https://doi.org/10.1016/j.neurobiolaging.2008.06.016.
Smith, E.E., Beaudin, A.E., 2018. New insights into cerebral small vessel disease and vascular cognitive impairment from Mri. Curr. Opin. Neurol. 31 (1), 36–43. https://doi.org/10.1097/WCO.0000000000000513.
Snowdon, D.A., Greiner, L.H., Mortimer, J.A., Riley, K.P., Greiner, P.A., Markesbery, W.R., 1997. Brain infarction and the clinical expression of Alzheimer disease. The Nun Study. J. Am. Med. Assoc. 277 (10), 813. https://doi.org/10.1001/jama.1997.03540340047031.
Song, X., Dhindsa, N., Rainey-Smith, S.R., Guo, H., Zeng, A., Brown, B.M., et al., 2017. Education and physical activity in relation to frailty and whole-brain structural health in Alzheimer's disease, mild cognitive impairment, and normal aging: results from the Australian imaging, biomarkers and lifestyle flagship study of ageing (AIBL). Alzheimer's Dement.: J. Alzheimer's Assoc. 13 (7), P639.
Soo, Y.O.Y., Yang, S.R., Lam, W.W.M., Wong, A., Fan, Y.H., Leung, H.H.W., et al., 2008. Risk vs benefit of anti-thrombotic therapy in ischaemic stroke patients with cerebral microbleeds. J. Neurol. 255 (11), 1679–1686.
Soontornniyomkij, V., Lynch, M.D., Mermash, S., Pomakian, J., Badkoobehi, H., Clare, R., Vinters, H.V., 2010. Cerebral microinfarcts associated with severe cerebral β-amyloid angiopathy. Brain Pathol. 20 (2), 459–467. https://doi.org/10.1111/j.1750-3639.2009.00322.x.
Squire, L.R., Zola-Morgan, S., 1991. The medial temporal lobe memory system. Science 253 (5026), 1380.
Stein, J.L., Medland, S.E., Vasquez, A.A., Derrek, P., Senstad, R.E., Winkler, A.M., et al., 2012. Identification of common variants associated with human hippocampal and intracranial volumes. Nat. Genet. 44 (5), 552–561. https://doi.org/10.1038/ng.2250.Identification.
Swan, G.E., DeCarli, C., Miller, B.L., Reed, T., Wolf, P.A., Carmelli, D., 2000. Biobehavioral characteristics of nondemented older adults with subclinical brain atrophy. Neurology 54 (11), 2108–2114. https://doi.org/10.1212/WNL.54.11.2108.
Takeda, S., Matsuzawa, T., 1985. Age-related brain atrophy: a study with computed tomography. J. Gerontol. 40 (2), 159–163.
Taki, Y., Goto, R., Evans, A., Zijdenbos, A., Neelin, P., Lerch, J., et al., 2004. Voxel-based morphometry of human brain with age and cerebrovascular risk factors. Neurobiol. Aging 25, 455–463. https://doi.org/10.1016/j.neurobiolaging.2003.09.002.
Thomas, A.J., O'brien, J.T., Davis, S., Ballard, C., Barber, R., Kalaria, R.N., Perry, R.H., 2002. Ischemic basis for deep white matter hyperintensities in major depression: a neuropathological study. Arch. Gen. Psychiatry 59 (9), 785–792.
Thomas, A.J., O'Brien, J.T., Barber, R., McMeekin, W., Perry, R., 2003. A neuropathological study of periventricular white matter hyperintensities in major depression. J. Affect. Disord. 76 (1), 49–54.
Tosto, G., Zimmerman, M.E., Carmichael, O.T., Brickman, A.M., 2014. Predicting aggressive decline in mild cognitive impairment: the importance of white matter hyperintensities. JAMA Neurol. 71 (7), 872–877.
Tullberg, M., Blennow, K., Månsson, J., Fredman, P., Tisell, M., Wikkelsö, C., 2007. Ventricular cerebrospinal fluid neurofilament protein levels decrease in parallel with white matter pathology after shunt surgery in normal pressure hydrocephalus. Eur. J. Neurol. 14 (3), 248–254.
Van Swieten, J.C., Van Den Hout, J.H., Van Ketel, B.A., Hijdra, A., Wokke, J.H.J., Van Gijn, J., 1991. Periventricular lesions in the white matter on magnetic resonance imaging in the elderly: a morphometric correlation with arteriolosclerosis and dilated perivascular spaces. Brain 114 (2), 761–774.
van Veluw, S.J., Shih, A.Y., Smith, E.E., Chen, C., Schneider, J.A., Wardlaw, J.M., et al., 2017. Detection, risk factors, and functional consequences of cerebral microinfarcts. Lancet Neurol. 16 (9), 730–740. https://doi.org/10.1016/S1474-4422(17)30196-5.
Varon, D., Barker, W., Loewenstein, D., Greig, M., Bohorquez, A., Santos, I., et al., 2015. Visual rating and volumetric measurement of medial temporal atrophy in the Alzheimer's Disease Neuroimaging Initiative (ADNI) cohort: Baseline diagnosis and the prediction of MCI outcome. Int. J. Geriatr. Psychiatry 30 (2), 192–200. https://doi.org/10.1002/gps.4126.
Vermeer, S.E., Koudstaal, P.J., Oudkerk, M., Hofman, A., Breteler, M.M.B., 2002. Prevalence and risk factors of silent brain infarcts in the population-based Rotterdam scan study participants and methods. Stroke 33 (1), 21–25.
Vermeer, S.E., Den Heijer, T., Koudstaal, P.J., Oudkerk, M., Hofman, A., Breteler, M.M.B., 2003a. Incidence and risk factors of silent brain infarcts in the population-based Rotterdam scan study. Stroke 32 (2), 392–396. https://doi.org/10.1161/01.STR.0000052631.98405.15.
Vermeer, S.E., Prins, N.D., Den Heijer, T., Hofman, A., Koudstaal, P.J., Breteler, M.M.B.B.,

2003b. Silent brain infarcts and the risk of dementia and cognitive decline. New England J. Med.(13). https://doi.org/10.1056/NEJMoa022066.
Vermeer, S.E., Longstreth, W.T., Koudstaal, P.J., 2007. Silent brain infarcts: a systematic review. Lancet Neurol. 6 (7), 611–619. https://doi.org/10.1016/S1474-4422(07)70170-9.
Vernooij, M.W., Ikram, M.A., Tanghe, H.L., Vincent, A.J.P.E., Hofman, A., Krestin, G.P., et al., 2007. Incidental findings on brain MRI in the general population. New England J. Med. 357 (18), 1821–1828.
Vernooij, M.W., van der Lugt, A., Ikram, M.A., Wielopolski, P.A., Niessen, W.J., Hofman, A., et al., 2008. Prevalence and risk factors of cerebral microbleeds the Rotterdam scan Study. Neurology 70 (14), 1208–1214.
Wahlund, L.O., Barkhof, F., Fazekas, F., Bronge, L., Augustin, M., Sjögren, M., et al., 2001. A new rating scale for age-related white matter changes applicable to MRI and CT. Stroke; J. Cereb. Circ. 32 (6), 1318–1322. https://doi.org/10.1161/01.STR.32.6.1318.
Walhovd, K.B., Fjell, A.M., Reinvang, I., Lundervold, A., Dale, A.M., Eilertsen, D.E., et al., 2005. Effects of age on volumes of cortex, white matter and subcortical structures. Neurobiol. Aging 26 (9), 1261–1270.
Wang, Y., Catindig, J.A., Hilal, S., Soon, H.W., Ting, E., Wong, T.Y., et al., 2012. Multi-stage segmentation of white matter hyperintensity, cortical and lacunar infarcts. NeuroImage 60 (4), 2379–2388. https://doi.org/10.1016/j.neuroimage.2012.02.034.
Wardlaw, J.M., Smith, E.E., Biessels, G.J., Cordonnier, C., Fazekas, F., Frayne, R., et al., 2013. Neuroimaging standards for research into small vessel disease and its contribution to ageing and neurodegeneration. Lancet Neurol. 12 (8), 822–838. https://doi.org/10.1016/S1474-4422(13)70124-8.
Wegner, C., Esiri, M.M., Chance, S.A., Palace, J., Matthews, P.M., 2006. Neocortical neuronal, synaptic, and glial loss in multiple sclerosis. Neurology 67 (6), 960–967.
Weller, R.O., Kida, S., Zhang, E., 1992. Pathways of fluid drainage from the brain-morphological aspects and immunological significance in rat and man. Brain Pathol. 2 (4), 277–284.
Weller, R.O., Hawkes, C.A., Kalaria, R.N., Werring, D.J., Carare, R.O., 2015. White matter changes in dementia: role of impaired drainage of interstitial fluid. Brain Pathology Vol. 25. pp. 63–78. https://doi.org/10.1111/bpa.12218.
Wen, W., Sachdev, P., 2004. The topography of white matter hyperintensities on brain MRI in healthy 60-to 64-year-old individuals. Neuroimage 22 (1), 144–154.
Werring, D.J., Frazer, D.W., Coward, L.J., Losseff, N.A., Watt, H., Cipolotti, L., et al., 2004. Cognitive dysfunction in patients with cerebral microbleeds on T2*-weighted gradient-echo MRI. Brain 127 (10), 2265–2275.
White, L., 2009. Brain lesions at autopsy in older Japanese-American men as related to cognitive impairment and dementia in the final years of life: a summary report from the Honolulu-Asia aging study. J. Alzheimer's Dis. 18 (3), 713–725.
World Health Organization, 2015. World Report on Ageing and Health. World Health Organization.
Wuerfel, J., Haertle, M., Waiczies, H., Tysiak, E., Bechmann, I., Wernecke, K.D., et al., 2008. Perivascular spaces - MRI marker of inflammatory activity in the brain? Brain 131 (9), 2332–2340. https://doi.org/10.1093/brain/awn171.
Yamashita, H., Fujikawa, T., Yanai, I., Morinobu, S., Yamawaki, S., 2002. Cognitive dysfunction in recovered depressive patients with silent cerebral infarction. Neuropsychobiology 45 (1), 12–18.
Zhang, Y., Brady, M., Smith, S., 2001. Segmentation of brain MR images through a hidden Markov random field model and the expectation-maximization algorithm. IEEE Trans. Med. Imaging 20 (1), 45–57.
Zhang, N., Song, X., Zhang, Y., Chen, W., DArcy, R.C.N., Darvesh, S., et al., 2011. An MRI brain atrophy and lesion index to assess the progression of structural changes in Alzheimers disease, mild cognitive impairment, and normal aging: a follow-up study. J. Alzheimer's Dis. 26 (3), 359–367. https://doi.org/10.3233/JAD-2011-0048.
Zhang, N., Song, X., Zhang, Y., 2012. Combining structural brain changes improves the prediction of Alzheimer's disease and mild cognitive impairment. Dement. Geriatr. Cogn. Disord. 33 (5), 318–326. https://doi.org/10.1159/000339364.
Zhu, Y.-C., Tzourio, C., Soumaré, A., Mazoyer, B., Dufouil, C., Chabriat, H., 2010. Severity of dilated Virchow-Robin spaces is associated with age, blood pressure, and MRI markers of small vessel disease: a population-based study. Stroke 41 (11), 2483–2490.